6-2000

Diastereoselection in titanium enolate addition to aldmines

Julia Leigh Barkin
Union College - Schenectady, NY

DIASTEREOSELECTION IN TITANIUM ENOLATE ADDITION TO ALDIMINES

By

Julia Leigh Barkin

****

Submitted in partial fulfillment

of the requirement for

Honors in the Department of Chemistry

UNION COLLEGE

June, 2000

Acknowledgements

I would like to thank Professor James C. Adrian Jr. for inspiring me to continue study in this field. Thank you for your infinite patience and confidence in me.

I would also like to show gratification to the Chemistry Department for supporting and encouraging my interest in chemistry and graduate school. I am grateful for all of the time and energy spent on me over the past four years.

Finally I would like to thank my family, friends and chem buddies for motivating me to accomplish my goals.

ABSTRACT

BARKIN, JULIA Diastereoselection in Titanium Enolate Addition to Aldimines. Department of Chemistry, June 2000.

A mild and versatile synthesis of α-oxy-ß-amino esters has been performed by condensation of the chlorotitanium enolates of methyl methoxyacetate with aldimines. The imine-aldol addition occurs in excellent yields without Lewis acid activation of the imine. All aryl imines examined show good to excellent diastereoselection for the anti isomers.

Table of Contents

Chapter			
I.	A.	Introduction	1
	B.	Electrophile Activation	3
	C.	Relative Stereochemistry	6
	D.	ß-Amino Ester Cyclization	9
	E.	Thesis Proposal	10
II.		Results	11
III.		Preliminary Kinetics	17
IV.		Discussion	18
V.		Experimental	21
VI.		References	41
VII.		Appendix	A1

Index of Figures

Contents

1. Taxol 1

2. ß-Amino Ester Cyclization 1

3. ß-Lactam Antibiotics 2

4. Imine-Aldol Reaction 2

5. Spectral Determination of Diastereoselection 14

6. Anti Crystal Structure 33g 15, 30

7. Syn Crystal Structure 33f 16, 35

8. Proposed Transition State 19

9. a) ^{1}H NMR of Ester 33a A1
   b) ^{13}C NMR of Ester 33a A2

10. a) ^{1}H NMR of Ester 33b A3
    b) ^{13}C NMR of Ester 33b A4

11. a) ^{1}H NMR of Ester 33c A5
    b) ^{13}C NMR of Ester 33c A6

12. a) ^{1}H NMR of Ester 33d A7
    b) ^{13}C NMR of Ester 33d A8

13. a) ^{1}H NMR of Ester 33e A9
    b) ^{13}C NMR of Ester 33e A10

14. a) ^{1}H NMR of Ester 33f A11
    b) ^{13}C NMR of Ester 33f A12

15. a) ^{1}H NMR of Ester 33g A13
    b) ^{13}C NMR of Ester 33g A14

16. a) ^{1}H NMR of Ester 33h A15
    b) ^{13}C NMR of Ester 33h A16

17. a) ^{1}H NMR of Ester 33i A17
b) ^{13}C NMR of Ester 33i A18

18. a) ^{1}H NMR of Ester 33j A19
b) ^{13}C NMR of Ester 33j A20

19. a) ^{1}H NMR of Ester 33k A21
b) ^{13}C NMR of Ester 33k A22

20. ^{1}H NMR of Representative Imine A23

Index of Tables

Contents

1. Effect of Variable Imine Substituents on Diastereoselection 12

2. Coupling Constants for the Two Diastereomer Signals of the α-Proton 14

3. HPLC Elution Gradients 21

4. Crystal Data and Structure Refinement for Ester 33g 30

5. Atomic Coordinates and Equivalent Isotropic Displacement Parameters for 33g 31

6. Bond Lengths and Angles for Ester 33g 32

7. Anistropic Displacement Parameters for Ester 33g 33

8. Hydrogen Coordinates and Isotropic Displacement Parameters for Ester 33g 34

9. Crystal Data and Structure Refinement for Ester 34f 35

10. Atomic Coordinates and Equivalent Isotropic Displacement Parameters for 34f 36

11. Bond Lengths and Angles for Ester 34f 37

12. Anistropic Displacement Parameters for Ester 34f 39

13. Hydrogen Coordinates and Isotropic Displacement Parameters for Ester 34f 40

A. Introduction

Synthesis of ß-amino esters is of current interest due to the pharmacological applications. Most notably, ß-amino esters appear in a range of natural products as well as serving as synthetic intermediates to other natural products.[1] The anti-cancer natural product Taxol, originally isolated from the bark of *Taxus brevifolia* contains an α-hydroxy-ß-amino ester moiety with syn relative stereochemistry (Figure 1).[2] The ß-amino ester moiety with this stereochemistry is necessary for biological anti-tumor activity.

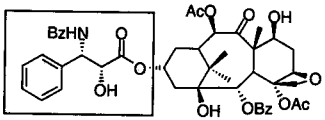

Figure 1. Taxol

In addition, ß-amino esters can serve as synthetic intermediates to 2-azetidinone rings as a result of intramolecular nucleophilic attack (Figure 2).[3]

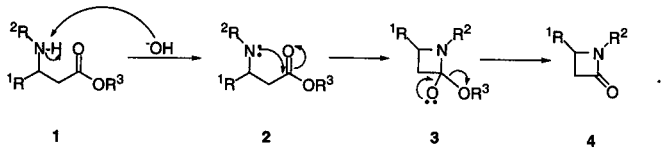

Figure 2. ß-Amino Ester Cyclization

In the presence of a base, the deprotonated amine (2) attacks the carbonyl carbon, eliminating the OR^3 portion of the ester functionality. The biological relevance of these four membered heterocycles is their antibiotic activity (Figure 3).[1] Examples of these

molecules are the ß-lactam family of antibiotics which include, among many others, Penicillin and Ampicillin.

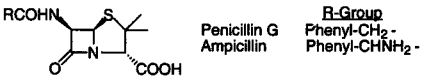

Figure 3. ß-Lactam Antibiotics

One synthetic approach to α-substituted ß-amino esters is the traditional aldol with an imine electrophile. Figure 4 illustrates an enolizable carbonyl compound (**5**) adding to an imine (**6**) resulting in the formation of a new carbon-carbon bond. This transformation further generates two new stereogenic centers circled in Figure 4 (**7**).

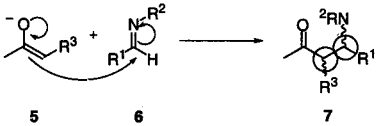

Figure 4. Imine-Aldol Reaction

B. Electrophile Activation

In the aldol-imine approach to ß-amino esters, one consideration is imine susceptibility to nucleophilic attack. Imines are often less susceptible to weak nucleophiles than their carbonyl counterparts. As a result they require some form of activation for addition to occur. Lewis acids are commonly used as electrophile activators.

In work done by Ojima and co-workers, a synthesis of ß-lactams is reported by reaction of silyl ketene acetals (**8**) with aldimines (**6**) promoted by titanium tetrachloride (Scheme 1). High yields of ß-lactam products (**10**) are afforded only in the presence of stoichiometric amounts of the Lewis acid activator $TiCl_4$.[4]

Scheme 1

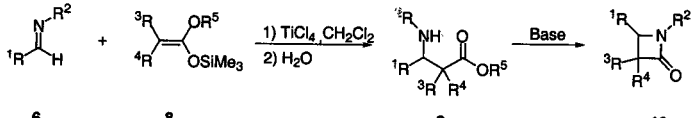

6 **8** **9** **10**

In more recent studies, Kobayashi and co-workers, using a zirconium catalyst, report the first catalytic addition of silyl ketene acetals (**11**) to aldimines (**6**), producing ß-amino esters (**12**) (Scheme 2).[5] Although both enolates of the two studies have the same

Scheme 2

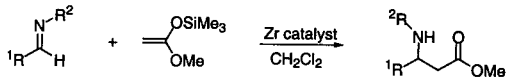

6 **11** **12**

nucleophilicity, there is a discrepancy as to the quantity of activator needed for addition.

In contrast to these studies, recent work by Cozzi and co-workers reports the addition of titanium enolates of 2-pyridyl thioesters (**13**) to aldimines (**6**) without the use of a Lewis acid for imine activation, affording moderate to good yields of the ß-lactam (**14**) products (Scheme 3).[6] These enolates which have predictably similar nucleophilicity

Scheme 3

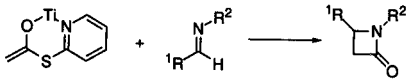

13 **6** **14**

to the silyl ketene acetals, require no additional equivalent of Lewis acid for activation. This raises the additional consideration that addition is possible without any need for activation of the electrophile.

In work done with titanium enolates of N-acyloxazolidinones by Wyatt and co-workers, Lewis acid activation in catalytic quantities is required for addition to aldimines.[7] These results in addition to the work of Cozzi suggest that the need for imine activation is dependant upon the nature of the enolate nucleophile.

In work done in our lab with chlorotitanium enolates (**15**), Lewis acid activated aldimines (**6**) are required for addition to occur to any extent (Scheme 4).[8] Without Lewis acid activation of the imine, yields are typically less than five percent. Yet, in the presence of an additional equivalent of Lewis acid, the addition is quantitative.

From this work and the literature cited, there is little conclusiveness as to the influence of imine activation in the imine-aldol synthesis. Further exploration into the nature of imine susceptibility to weak nucleophiles is of great interest in our lab.

Scheme 4

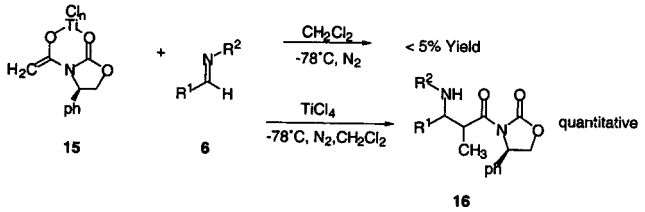
Cln
Ti
H2C
ph
15
+
R2
N
R1
H
6
CH2Cl2
-78°C, N2
< 5% Yield
TiCl4
-78°C, N2,CH2Cl2
R2
NH
R1
CH3
ph
quantitative
16

C. Relative Stereochemistry

Further consideration in the aldol-imine approach to α-substituted-ß-amino esters is the stereochemical outcome. For the two stereocenters of the amino ester, circled in Figure 4, bearing the amine and the methoxy groups, there are two possible relative configurations, which are the anti and syn diastereomers. In addition there is the absolute stereochemistry of each stereocenter, or R and S designation. We are primarily interested in the diastereoselection of aldol type synthesis although studies involving chiral Lewis acids are of interest for future work.

In previous work done by Cozzi and co-workers, chlorotitanium enolates of thioesters (**17** & **17a**) in an aldol addition yields mixtures of the two diastereomeric products (**19** & **20**).[9] Interestingly, when the ether of the thioester (**16**) is a larger *t*-butyldimethylsilyl (TBDMS) group, the syn product (**20**) predominates while the smaller benzyl ether results in a diastereomeric excess of the anti product (**19**) (Scheme 5).

Scheme 5

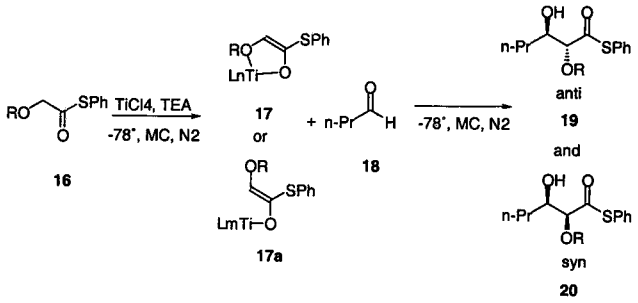

Cozzi explains this outcome with two possible enolates. The benzyl ether forms a bidentate Z-enolate (**17**) which results in an excess of the anti product, while the TBDMS

ether forms a monodentate enolate (**17a**) resulting in an excess of the syn product. Both are suggested to proceed through a cyclic boat-like transition state.

Further complication arises when enolates are added to imines due to involvement of the nitrogen substituent of the imine. There is the possibility of steric and electronic interaction between this substituent and the nucleophile, which can influence the stereochemical outcome. The following studies present precedent for diastereoselective imine-aldol additions.

In work done by Wyatt and co-workers, titanium enolates of N-acyloxazolidinones (**21**) when added to benzaldimines (**22**) show good selectivity for the anti diastereomer (**23** & **23a**) (Scheme 6).[7] In this work, diastereoselection is intrinsic upon chiral reagents. Wyatt suggests a number of possible transition structures, which correspond to the two diastereomers. Proposed is a range of possible chelated and non-chelated states resulting in either of the two diastereomers.

Scheme 6

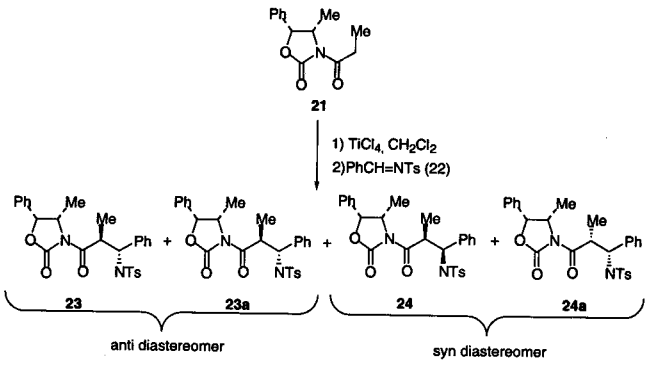

In other work with imines, Fujisawa and co-workers find that addition of metal ester enolates of propionate and butyrate results in a mixture of diastereomers (**27** & **28**) (Scheme 7). They report that by varying the metal center of the enolate, they can control the resulting stereochemistry of the product ß-lactams. With titanium enolates they find that the stereochemical outcome can further be manipulated by changing the steric bulkiness of the R substituents of the chiral imine. The R substituent with larger steric bulk results in less stereoselection while the smaller R substituents show excellent stereoselection. This is rationalized through a chair-like transition state in which the titanium, unlike lithium, does not chelate to the imine R substituent suggesting that it is the bulk of these substituents which is deterring addition to the *re*-face.[10] Similar to the

Scheme 7

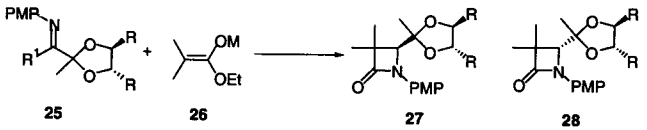

25 **26** **27** **28**

PMP = *p*-methoxyphenyl
M = metal

work done by Wyatt, the stereochemical outcome is dependant upon the chirality and steric bulk of the imine substituents.

D. ß-Amino Ester Cyclization

One additional consideration in the imine-aldol approach is the possible cyclization of the ß-amino ester to the ß-lactam under the basic conditions required for enolization. From previous work done in our lab, we discovered that an orthomethoxyphenyl nitrogen substituent of the aldimine, directs for the ß-amino ester product over the ß-lactam.[11] This is attributed to the inductive effect of this substituent on the nitrogen, which impedes cyclization. This substituent is of particular interest as

Scheme 8

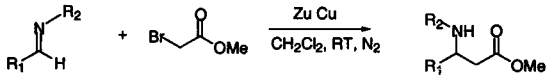

28 **29** **30**

R_2 = *ortho*-methoxyphenyl

well due to ease of removal over other forms of activation, to afford the resulting amine with ceric ammonium nitrate (CAN).

E. Thesis Proposal

In the report following we are first interested in examining the role of Lewis acids in the nucleophilic addition of the chlorotitanium enolate (**32**) of a methyl ester (**31**) to imines (**6**) (Scheme 9). Chlorotitanium enolates of methyl methoxyacetate are relatively weak nucleophiles suggesting the need for Lewis acid activation of the imine in either stoichiometric, as seen in Ojima's work with silyl ketene acetals, or possibly catalytic quantities. The work by Cozzi suggests that indeed possibly no Lewis acid is needed for imine activation. The variability of imine activation required in the literature for weak nucleophiles makes predictions for this approach very difficult.

Scheme 9

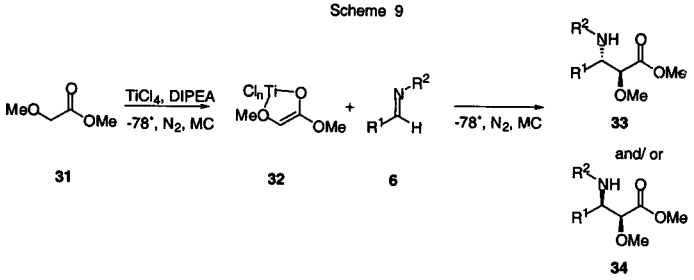

31 **32** **6** **33** **34**

In addition, the work that has been done previously is focused on aldol stereoselective synthesis with insufficient exploration of stereoselective imine-aldol reactions. Previously reported diastereoselective imine-aldol synthesis often require chiral reagents to achieve stereoselection. We set out to determine the nature of reactivity and selectivity of this mild approach to α-substituted-ß-amino esters.

Results

We have developed a highly effective preparation of α-oxy-ß-amino esters, which is both diastereoselective and nearly quantitative (Scheme 9). Further, this method does not require any Lewis acid imine activation.

Scheme 9

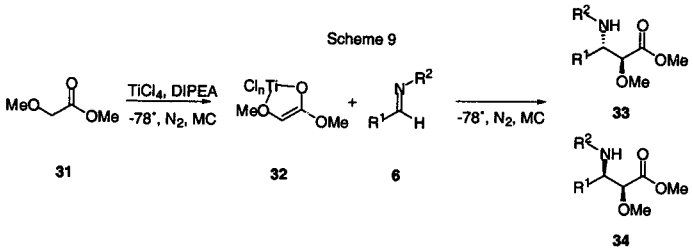

The chlorotitanium enolates (**32**) of methyl methoxyacetate (**31**), prepared according to the method of Evans[12], are added to a number of different aryl substituted imines (**6**). Imines are prepared by condensation of the corresponding amines and aldehydes. In the first six entries in Table 1, we add the enolates to imines prepared from benzaldehyde and varying amines.

For esters 33c, 33d, and 33e seen in the table, the diastereoselection is good, ranging from 74:26 to 78:22 in favor of the anti product. Both 33c, and 33d are para substituted while 33e has an unsubstituted phenyl nitrogen substituent. Esters 33a, 33b, and 33f show excellent diastereoselection, greater than 90:10 in favor of the anti product. All of these esters have ortho substituted nitrogen substituents. Esters 33a and 33f with high electron donating ability of the phenyl substituent have similar selectivity to the less donating ethyl substituted phenyl ring.

Table 1. Effect of Variable Imine Substituents on Diastereoselection

entry	R^2	R^1	d.r. (a:s)	Yield (%)[a]
33 a	*o*-Clph[c]	ph	97:3[b]	83
33 b	*o*-ethph[d]	ph	91:9	73
33 c	PMP[e]	ph	74:26	77
33 d	*p*-NO_2ph[f]	ph	77:23[b]	52
33 e	ph[g]	ph	78:22	70
33 f	OMP[h]	ph	94:6	63
33 g	OMP	*p*-Clph	96:4	95
33 h	OMP	PMP	94:6	84
33 i	OMP	*p*-Meth[i]	92:8	68
33 j	OMP	napthyl	91:9	87
33 k	OMP	furanyl	93:7	50
33 l	OMP	*tert*-Bu	-	NR

[a] Isolated Yield, [b]Determined by ^{1}H NMR of the crude reaction mixture, [c]*ortho*-chlorophenyl, [d]*ortho*-ethylphenyl, [e]*para*-methoxyphenyl, [f]*para*-nitrophenyl , [g]phenyl, [h]*ortho*-methoxyphenyl, [i]*para*-methylphenyl

As a result of the high stereoselection of the products with ortho substituted nitrogen substituents, we subsequently prepare imines from an *ortho*-aniline amine and a variety of aryl aldehydes. As previously mentioned, the *ortho*-methoxyphenyl substituent is of particular interest due to the ease at which it can be removed from the product.[11] We have also found from previous work that this substituent leads solely to the ß-amino ester product via the addition of (methoxycarbonyl)methyl zinc bromide to aldimines derived from *ortho*-methoxyaniline.[11]

In entries 33f – 33k corresponding to the esters of the same designation, when the nitrogen substituent is an *ortho*-methoxyphenyl ring and the R^1 substituent is varied, the diastereoselection is excellent in favor of the anti product. Examining the influence of R^1 size upon the stereoselection, the larger napthyl (33j) and the smaller furanyl (33k) have similar selectivities of 91:1 and 93:7 respectively. The esters with para substituted phenyl R^1 substituents, entries 33g, 33h and 33i, show excellent diastereoselectivity as

well, seemingly independent of the phenyl substituent identity. The products with the highly electron donating *para*-methoxyphenyl carbon substituent, 33h, as well as the methyl substituted phenyl substituent, 33i, have diastereoselectivies of 94:6 and 92:8 respectively in favor of the anti product.

We examined one alkyl imine (33l), with a *tert*-b utyl carbon substituent, which does not appear to react with the enolate to any extent. This suggests that this chemistry in ineffective with non-enolizable alkyl imines and is limited to aryl imines Further attempts to isolate alkyl imines have been unsuccessful to date.

Reported diastereomeric ratios of the products are determined by HPLC and ^{1}H NMR. In the ^{1}H NMR, the diastereomeric ratios are extracted from the signal integration of the proton alpha to the carbonyl. For one representative ester, 33e, this is the proton on the carbon center circled in the structure in Figure 5. The portion of the ^{1}H NMR spectra seen in Figure 5 shows the two doublets of the major and minor diastereomers (a:s = 78:22). The HPLC UV spectra for ester 33e on the right side of Figure 5, shows two signals with an elution time approximately half of a minute apart for the two diastereomers. A ratio of the area under the two peaks affords a diastereomeric ratio (a:s = 78:22) in agreement with the ratio determined by ^{1}H NMR. Two products, 33a (Figure 9a, A1) and 33d (Figure 12a, A4) have diastereomers which elute simultaneously so that ^{1}H NMR is used exclusively to determine the diastereomeric ratio.

In all cases except for one, the signals for the major diastereomer fall down field from the minor. For ester 33k, the syn signals are shifted slightly downfield of the anti signals (Figure 19a, A21). The coupling of the major diastereomer for each of the esters

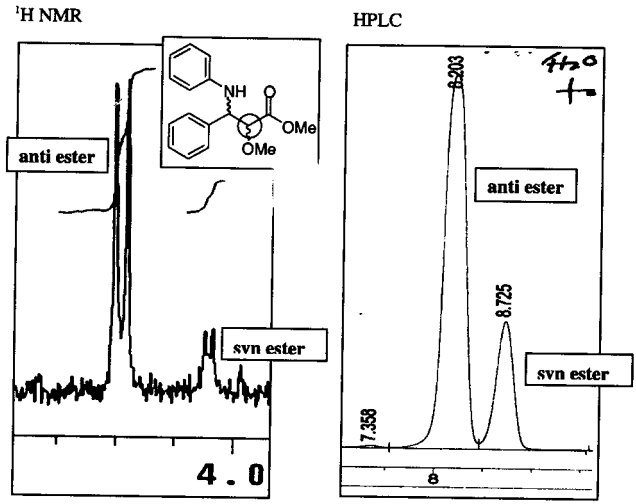

Figure 5. Spectral Determination of Diastereoselection

is larger than minor ester coupling. Table 2 shows a comparison of coupling and chemical shift for the two diastereomers of each of the esters. In some cases where the minor diastereomer accounts for less than ten percent of the ester product mixture, minor coupling is indistinguishable.

Table 2. Coupling Constants for the Two Diastereomer Signals of the α-Proton

	Ester->	33a	33b	33c	33d	33e	33i	33j	33k
Anti	Shift/ppm	4.20	4.19	4.20	4.21	4.19	4.19	4.28	4.21
	Coupling/Hz	5.0	4.0	5.0	5.0	4.0	5.0	5.0	4.0
Syn	Shift/ppm	4.08	4.08	4.03	4.07	4.03	4.03	4.15	4.30
	Coupling/Hz	3.0	2.0	3.0	3.0	3.0	2.0	4.0	1.0

We were able to isolate defractable crystals for the major and minor isomers of two esters. Figures 6 and 7 show the crystal structures for the major product of 33g, which has anti relative stereochemistry and the minor product of 33f, with syn relative stereochemistry.

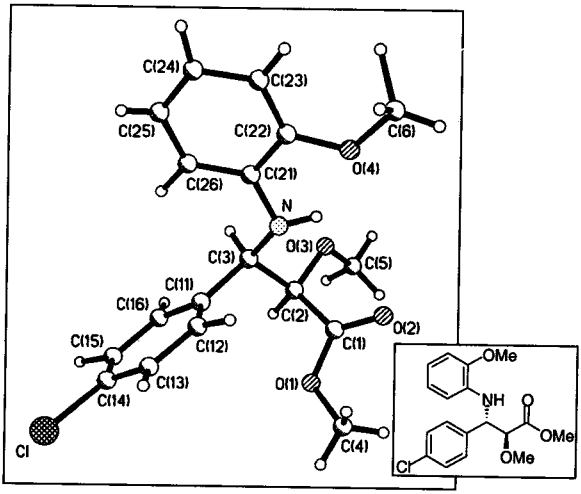

Figure 6. Anti Crystal Structure 33g

Isolated yields are typically 70% to 90% with less than 5% impurities. Slightly lower yields are afforded for the *para*-nitro substituted phenyl R^2 substituted product (33d) as well as the furanyl R^1 substituted ester (33k).

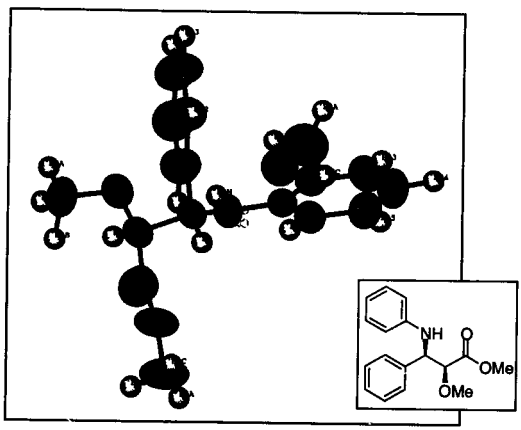

Figure 7. Syn Crystal Structure 33f

Preliminary Kinetics

In addition we attempted some preliminary work into the reaction kinetics of the enolate addition to the aldimine. We used the reaction seen in Scheme 9 to make product 33c. Five microliter aliquots were taken at five minute intervals for one hour after cannulation of the enolate into a stirred solution of imine in methylene chloride. The aliquots were quenched with 2.0 mL of an acetonitrile/water 50:50 mixture. They were then analyzed by high pressure liquid chromatography. Four peaks were present in the HPLC from the imine, aldehyde, and the two products. A comparison of the peak areas for the ester and reagent signals over the time intervals, suggests that the addition is complete within 5-10 minutes of addition of the enolate.

Discussion

A highly diastereoselective synthesis for ß-amino esters was developed based on the traditional aldol approach with an imine electrophile. This procedure, which is nearly quantitative, does not require any Lewis acid imine activation. The crude and purified products are extremely clean with generally less than 5% impurities.

Additional equivalents of Lewis acid show no noticeable increase in selectivity or yield. Stiochiometric and catalytic quantities of Lewis acid added to the imine, are equally selective and high yielding without any additional Lewis acid. This suggests that the chlorotitanium enolate nucleophile, which we use, has sufficient nucleophilicity to result in addition. Interestingly, addition of Lewis acids of alternative metals than titanium to the imine, such as tin, result in less diastereoselection for the anti product. This is perhaps due to metal exchange of the titanium from the enolate, with the metal intended for imine activation.

The extent of diastereoselectivity for the anti product is dependent upon the nitrogen substituent of the imine. When the substituent in the ortho position to the nitrogen on the phenyl ring is other than a hydrogen, diastereoselectivity is excellent. Phenyl substituents with para substitution or without substitution show good diastereoselection. This suggests that there is favorable interaction for stereoselection between an ortho substituted ring and the enolate in the transition structure.

We propose one enolate which proceeds through two nondegenerate transition states (Figure 8). Both the monodentate and bidentate enolates have Z-configuration due to the priority of the metal bound oxygen. The enolate is in a fast equilibrium between the chelated and non-chelated states. From our results, the more favorable and lower

energy transition state leads to the anti product while the syn product is reached through a higher energy, less favorable transition state. We therefore propose a Zimmerman-Traxler chair-like transition state for the lower energy anti transition state, while a higher energy boat-like transition state leads to the syn product.[13]

Due to the steric bulk of the two aryl substituents of the imine, it exists in the E conformation. This is confirmed in the ^{1}H NMR in which there are clearly one set of signals in the spectra for each of the imines (representative imine, Figure 20, A23).

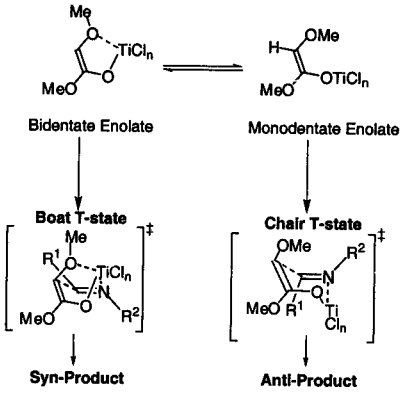

Figure 8. Proposed Transition State

In the two suggested transition states, the imine is situated with one of the two faces approaching the enolate. The state resulting in the anti product has the monodentate enolate approaching the imine with the R^2 substituent is in a pseudo equatorial position situated above the ring in the formation (Figure 8). The state resulting in the syn product

has the bidentate enolate approaching the imine with the R^2 substituent situated below the boat-like ring in a pseudo-equatorial position.

Stereochemical influence in the starting materials is not needed to observe excellent diastereoselection in chlorotitanium enolate addition to aldimines. Unlike previous work, there is no stereochemical directing influence of the reagents in our approach and the resulting products are highly diastereoselective. This is an advantageous platform from which to approach enantioselective addition with chiral Lewis acids.

Experimental

General.

^{1}H NMR are recorded on a Varian-200 spectrometer. All samples are dissolved in $CDCl_3$. Chemical shifts are reported in ppm from tetramethylsilane (TMS) with the solvent resonance as the internal standard (deuterochloroform: δ 7.26 ppm). ^{13}C NMR are also recorded on a Varian-200 spectrometer with complete proton decoupling. IR is performed on a Perkin Elmer 1600 series FTIR instrument. Thin Layer Chromatography (TLC) is performed using Whatman K6F Silica Gel 60A (0.25 mm) analytical glass plates. Fisher silica gel 60A (200-425 mesh) is used for flash chromatography which is performed according to the method of Still.[14]

Analytical high performance liquid chromatography is carried out on a Hewlett-Packard HP 1100 Chromatograph on a Zorbax SB-C18 4.6 mm x 25 mm column. A variety of solvent gradients (Table 3) are used to achieve diastereomer separation. All flow rates are one mL/min.

Table 3. HPLC Elution Gradients

Gradient	% ACN at Start	% ACN at End	Gradient Time (min)
1	55	65	9
2	55	65	11
3	55	65	13
4	40	70	13

All enolate reactions are run under N_2 with distilled solvent dichloromethane (CH_2Cl_2). Dichloromethane is distilled from calcium hydride. All other commercially available reagents and solvents were reagent grade and used without further purification unless otherwise noted. Enolates were reacted with imines for 1hour unless otherwise indicated. Formation of titanium enolates was allowed 1 hour in all cases.

All diastereomeric ratios are presented as anti:syn.

Typical Procedures.

Preparation of Imine: To a stirred solution of the aniline derivative (23.0 mmol) and the aldehyde (23.0 mmol) in toluene was added approx. 4 g of 4 Å molecular sieves. After 24 hours the solution was vacuum filtered, and concentrated *in vacuo* to afford a quantitative amount of the imine. If the imine was an oil, no further purification was performed. If the resulting imine was a solid, it was recrystalized.

Methyl 3-(2-methoxyphenyl)amino-2-methoxy-3-(4-methoxy)phenyl propanoate (33h). To a stirred solution of methyl methoxyacetate (1) (2 mmol) in CH_2Cl_2 (6.0 mL) cooled at -78 °C was added, dropwise, 2.1 mL of a 1.0 M solution of $TiCl_4$ in CH_2Cl_2 (2.1 mmol). After 5 minutes, diisopropylethylamine (400 µl, 2.2 mmol) was added dropwise affording a blue solution indicative of enolate formation. After 1 hour the enolate solution was transferred via cannula to a stirred solution of aldimine (1.0 mmol) in CH_2Cl_2 at -78 °C. After 1 hour the reaction was quenched with the addition of approx. 10.0 mL of a 1 M HCl solution. The organic phase was separated, washed sequentially with 25 mL of water and brine, dried with $MgSO_4$ and concentrated *in-vacuo* to afford 0.399 g of a yellow oil, which was chromatographed to afford 0.303 g (84 %) of a yellow oil. The diastereomeric ratio was determined to be 94:6 (anti:syn). Rf = 0.19 (SiO_2, 5 % Et_2O/CH_2Cl_2); IR (Thin Film); 3419, 2924, 2853, 1750, 1601, 1511, 1457, 1248, 1247, 1177, 1129, 1028, 740 cm^{-1}; 200 MHz ^1H NMR; δ 7.23 (d, 2H, J = 7.0), 6.83-6.73 (m, 5H), 6.45 (dd, 1H, J = 7.0 Hz, J = 2.0 Hz), 5.30 (d, 1H, J = 8.0 Hz), 4.80 (dd, 1H J = 8.0 Hz, J = 5.0 Hz), 4.18 (d,

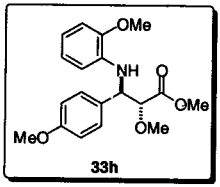

33h

1H, J = 5.0), 3.89 (s, 3H), 3.76 (s, 3H), 3.67 (s, 3H), 3.44 (s, 3H); 50 MHz ^{13}C NMR; δ 170.9, 159.1, 147.2, 136.2, 130.3, 128.6, 121.1, 117.1, 113.8, 111.5, 109.6, 83.7, 56.2, 58.4, 55.5, 55.1, 51.9. HPLC (gradient #1, flow rate = 1.0 mL/min): t_R = 8.8 min (major diastereomer), t_R = 9.2 min (minor diastereomer).

Physical Data for the ß-amino ester derivatives are as follows:

Methyl 3-(2-chlorophenyl)amino-2-methoxy-3-phenylpropanoate (33a). Reaction

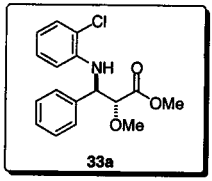

33a

time = 12 h. The crude product is a brown oil and isolated as a yellow oil, isolated yield: 83%: Rf = 0.17 (SiO_2, 25 % Hexane/CH_2Cl_2); IR (Thin Film); 3403, 3064, 3030, 3000, 2951, 2930, 2834, 1754, 1597, 1501, 1453, 1434, 1356, 1322, 1272, 1203, 1127, 1034, 1006, 816, 744, 700 cm^{-1}; 200 MHz ^{1}H NMR; δ 7.32-7.26 (m, 6H), 6.98 (dt, 1H, J= 7.0 Hz, J = 1.0 Hz), 6.59 (dt, 1H, J= 7.0 Hz, J = 1.0 Hz), 6.47 (dd, 1H, J = 8.0 Hz, J = 5.0 Hz), 5.53 (d, 1H, J = 8.0 Hz), 4.86 (dd, 1H J = 8.0 Hz, J = 5.0 Hz), 4.20 (d, 1H, J = 5.0 Hz), 3.67 (s, 3H), 3.46 (s, 3H); ^{13}C NMR ($CDCl_3$): δ 170.5, 142.3, 137.6, 129.1, 128.5, 128.0, 127.7, 127.4, 119.8, 117.9, 112.7, 83.5, 59.3, 58.9, 52.0; HRMS, calcd for $C_{17}H_{16}ClNO_3$ 319.0970, found 319.0968.

Minor isomer 34a (syn) *CH*(OMe) signal: 200 MHz ^{1}H NMR; δ 4.08 (d, J = 3.0 Hz).

Methyl 3-(2-ethylphenyl)amino-2-methoxy-3-phenylpropanoate (33b).

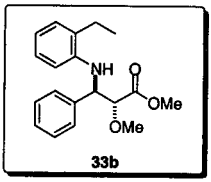

33b

The crude product is a brown oil and isolated as a yellow oil, isolated yield: 73%: Rf = 14.5 (SiO_2, 25 % Hexane/ CH_2Cl_2); IR (Thin Film); 3429, 3063, 3029, 2962, 2930, 2874, 1743, 1605, 1587, 1510, 1454, 1354, 1304, 1270, 1202, 1126, 1027, 748, 702 cm^{-1}; 200 MHz ^1H NMR; δ 7.35-7.26 (m, 5H), 7.08-6.91 (m, 2H), 6.69-6.61 (m, 1H), 6.4 (dd, 1H, J = 8.0 Hz, J = 1.0 Hz), 4.87 (s, 1H), 4.19 (d, 1H, J = 4.0 Hz), 3.62 (s, 3H), 3.43 (s, 3H), 2.61 (q, 2H, J = 7.0 Hz), 1.31 (t, 3H, J = 7.0 Hz); 50 MHz ^{13}C NMR; δ 170.9, 143.8, 138.5, 128.5, 128.2, 128.0, 127.8, 127.3, 126.9, 117.6, 111.5, 83.7, 59.1, 59.0, 51.9, 24.2, 13.0; HRMS, calcd for $C_{19}H_{23}NO_3$ 313.1678, found 313.1678. HPLC (gradient # 3): t_R = 11.7 min (major diastereomer), t_R = 12.0 min (minor diastereomer); **Minor isomer 34b (syn) C*H*(OMe) signal:** 200 MHz ^1H NMR; δ 4.08 (d, J ≤ 2.0 Hz).

Methyl 3-(4-methoxyphenyl)amino-2-methoxy-3-phenylpropanoate (33c). The crude

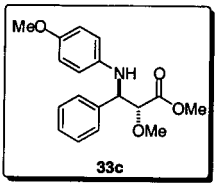

33c

product is a brown oil which slowly crystallizes and isolated as a pale yellow oil which slowly crystallizes, isolated yield: 77%: mp = 84 - 86 °C; Rf = 0.26 (SiO_2, 2.5/37.5/60% ether/Hexane/CH_2Cl_2); IR (Thin Film); 3391, 3029, 2996, 2951, 2833, 1752, 1513, 1454, 1242, 1197, 1127, 1036, 822, 756, 703 cm^{-1}; 200 MHz ^1H-NMR; δ 7.36-7.23 (m, 5H), 6.70 (d, 2H, J = 9.0 Hz), 6.57 (d, 2H, J = 9.0 Hz), 4.75 (d, 1H, J = 5.0 Hz), 4.20 (d, 1H, J = 5.0 Hz), 3.69 (s, 3H), 3.62 (s, 3H), 3.44 (s, 3H); 50 MHz ^{13}C-NMR; δ 170.8, 152.3, 140.6, 138.2, 128.4, 127.8, 127.4, 115.5, 114.7,

83.4, 60.2, 59.0, 55.6, 51.8; An analytical sample was recrystallized from 95% ethanol as white needles, analysis calcd for $C_{18}H_{21}NO_4$: C, 68.55; H, 6.71; N, 4.44; found : C, 68.69; H, 6.79; N, 4.37; HRMS, calcd for $C_{18}H_{21}NO_4$ 315.1471, found 315.1471. HPLC (gradient # 3): t_R = 7.1 (major diastereomer), t_R = 7.8 (minor diastereomer). **Minor isomer 34c (syn) C*H*(OMe) signal:** 200 MHz ^{1}H NMR; δ 4.03 (d, J = 3.0 Hz).

Methyl 3-(4-nitrophenyl)amino-2-methoxy-3-phenylpropanoate (33d). The crude

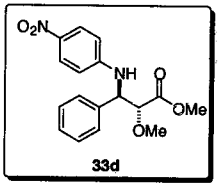

33d

product is a brown oil and isolated as a yellow/orange oil, isolated yield: 52%; Rf = 0.20 (SiO_2, 5 % Hexane/CH_2Cl_2); IR (Thin Film); 3476, 3373, 3083, 2922, 2851, 1744, 1599, 1502, 1478, 1309, 1183, 1112, 838 cm^{-1}; 200 MHz ^{1}H NMR; δ 8.01 (d, 2H, J = 9.0 Hz), 7.30 (m, 5H), 6.52 (d, 2H, J = 9.0 Hz), 5.70 (d, 1H, J = 7.0 Hz), 4.90 (dd, 1H, J = 7.0 Hz, J= 5.0 Hz), 4.21 (d, 1H, J = 5.0 Hz), 3.61 (s, 3H), 3.49 (s, 3H); 50 MHz ^{13}C NMR; δ 170.9, 151.8, 138.8, 136.5, 128.8, 128.5, 127.2, 126.1, 112.2, 82.7, 59.0, 58.6, 52.0; HRMS, calcd for $C_{17}H_{18}N_2O_5$ 330.1216, found 330.1208. **Minor isomer 34d (syn) C*H*(OMe) signal:** 200 MHz ^{1}H NMR; δ 4.07 (d, J = 3.0 Hz).

Methyl 3-phenylamino-2-methoxy-3-phenylpropanoate (33e). The crude products are

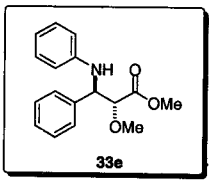

33e

a yellow/brown solid, the isolated products are a pale yellow crystalline solid, isolated yield: 70%. mp = 73-75 °C; Rf = 0.16 (SiO_2, 25 % Hexane/CH_2Cl_2); IR (Thin Film); 3401, 3025, 2923, 2852, 1743, 1603, 1505, 1453, 1434, 1356, 1272, 1200, 1127, 1028, 750 cm^{-1}; 200 MHz ^{1}H NMR; δ 7.33-7.23 (m, 5H), 7.10 (t, 2H, J

= 8.0 Hz), 6.67 (t, 1H, J = 8.0 Hz), 6.89 (d, 2H, J = 8.0 Hz), 4.82 (bd, 2H, J = 4.0 Hz), 4.19 (d, 1H, J = 4.0 Hz), 3.62 (s, 3H), 3.45 (s, 3H); 50 MHz ^{13}C NMR; δ 170.9, 146.5, 148.2, 129.2, 128.5, 127.9, 127.4, 118.0, 114.0, 83.4, 59.2, 59.0, 51.9; Analysis calcd for $C_{17}H_{19}NO_3$: C, 71.56; H, 6.71; N, 4.91; found : C, 71.38; H, 6.64; N, 4.77; HPLC (gradient # 3): t_R = 8.2 (major diastereomer), t_R = 8.7 (minor diastereomer); **Minor isomer 34e (syn) C*H*(OMe) signal:** 200 MHz ^{1}H NMR; δ 4.03 (d, J = 3.0 Hz).

Methyl 3-(2-methoxyphenyl)amino-2-methoxy-3-phenylpropanoate (33f). The crude

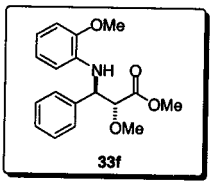

33f

product is a brown oil and isolated as a brown oil, isolated yield: 95%. Rf = 0.12 (SiO_2, 30% hexane/CH_2Cl_2); IR (Thin Film); 3416, 2999, 2951, 2835, 1744, 1602, 1513, 1456, 1348, 1223, 1128, 1027, 739, 703 cm^{-1}; 200 MHz ^{1}H NMR; δ 7.31-7.21 (m, 5H), 6.78-6.58 (m, 3H), 6.45 (dd, 1H, J = 7.0 Hz, J= 2.0 Hz), 4.75 (bs, 1H), 4.83 (d, 1H, J = 5.0 Hz), 4.21 (d, 1H, J = 5.0 Hz), 3.89 (s, 3H), 3.65 (s, 3H), 3.44 (s, 3H); 50 MHz ^{13}C NMR; δ 170.8, 147.2, 138.4, 136.2, 128.4, 127.8, 127.5, 121.1, 117.2, 111.4, 109.6, 83.7, 59.1, 59.0, 55.5, 51.8; HRMS, calcd for $C_{18}H_{21}NO_4$ 315.1471, found 315.1479. HPLC (gradient #4): t_R = 7.1 (major diastereomer), t_R = 7.8 (minor diastereomer). **Minor isomer 34f (syn)** spontaneously crystallized from the crude mixture; 200 MHz ^{1}H NMR; δ 7.39-7.22 (m, 5H), 6.77-6.55 (m, 3H), 6.32 (dd, 1H, J = 7.0 Hz, J= 2.0 Hz), 5.36 (d, 1H, J = 8.0 Hz), 4.75 (dd, 1H, J = 8.0 Hz, J = 3.0 Hz), 4.06 (d, 1H, J = 3.0 Hz), 3.88 (s, 3H), 3.71 (s, 3H), 3.34 (s, 3H).

Methyl 3-(2-methoxyphenyl)amino-2-methoxy-3-(4-chloro)phenylpropionate (33g).

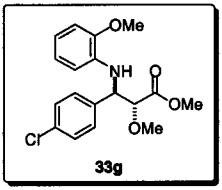

33g

The crude product is a brown oil which slowly crystallizes and isolated as a pale yellow oil which slowly crystallizes, isolated yield: 95%; mp: 99-101 °C; Rf = 0.23 (SiO_2, 40% hexane/CH_2Cl_2); IR (Thin Film); 3416, 3000, 2951, 2834, 1753, 1602, 1513, 1457, 1244, 1223, 1128, 1028, 910, 736 cm^{-1}; 200 MHz ^1H NMR; δ 7.25 (s, 4H), 6.79-6.61 (m, 3H), 6.40, (dd, 1H, J = 7.0 Hz, J = 2.0 Hz), 5.31 (d, 1H, J = 8.0 Hz), 4.81 (dd, 1H, J = 8.0 Hz, J = 5.0 Hz), 4.19 (d, 1H, J = 5.0 Hz), 3.89 (s, 3H), 3.68 (s, 3H), 3.45 (s, 3H); 50 MHz ^{13}C NMR; δ 170.5, 147.1. 136.9, 135.7, 133.4, 128.8, 128.4, 121.0, 117.4, 111.4, 109.5, 83.3, 59.1, 58.3, 55.5, 51.9; Analysis calcd for $C_{18}H_{20}NO_4Cl$: C, 61.80; H, 5.76; N, 4.00; found : C, 61.78; H, 5.86; N, 3.91; HPLC (gradient #3): t_R = 125 (major diastereomer), t_R = 13.5 (minor diastereomer). **Minor isomer 34g (syn)** spontaneously crystallized from a dilute 95% ethanol solution; mp: 163-164 °C; 200 MHz ^1H NMR; δ 7.32 (d, 2H, J = 9.0 Hz), 7.26 (d, 2H, J = 9.0 Hz), 6.78-6.58 (m, 3H), 6.28, (dd, 1H, J = 8.0 Hz, J = 2.0 Hz), 5.34 (d, 1H, J = 8.0 Hz), 4.85 (dd, 1H, J = 8.0 Hz, J = 3.0 Hz), 4.02 (d, 1H, J = 3.0 Hz), 3.88 (s, 3H), 3.73 (s, 3H), 3.35 (s, 3H).

Methyl 3-(2-methoxyphenyl)amino-2-methoxy-3-(4-methyl)phenylpropanoate (33i).

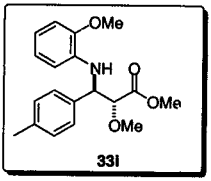

33I

The crude product is a brown oil and isolated as a light brown oil which slowly crystallizes. Isolated yield: 95%; mp: 83-85 °C; Rf = 0.17 (SiO_2, 25% hexane/CH_2Cl_2); IR (Thin Film); 3416, 3000, 2950, 2926, 2834, 1755, 1602, 1513, 1456, 1432, 1346, 1244, 1223, 1128, 1027, 738 cm^{-1}; 200 MHz ^1H NMR; δ 7.19 (d, 1H, J = 8.0 Hz), 7.07 (d, 1H, J = 8.0 Hz), 6.78-6.58 (m, 3H), 6.45 (dd, 1H, J = 7.0 Hz, J = 2.0 Hz), 5.32 (d, 1H, J = 7.0 Hz), 4.80 (dd, 1H, J = 7.0 Hz, J = 5.0 Hz), 4.19 (d, 1H, J = 5.0 Hz), 3.88 (s, 3H), 3.67 (s, 3H), 3.43 (s, 3H), 2.28 (s, 3H); 50 MHz ^{13}C NMR; δ 170.8, 147.0, 137.1, 136.1, 135.1, 129.0, 127.2, 121.0, 116.9, 111.3, 109.4, 83.6, 59.0, 58.5, 55.4, 51.7, 21.0; HRMS, calcd for $C_{19}H_{23}NO_4$ 329.1627, found 329.1621; HPLC (gradient #3): t_R = 10.7 (major diastereomer), t_R = 11.5 (minor diastereomer); An analytical sample was recrystallized from 95% ethanol as colorless prisims, analysis calcd for $C_{19}H_{23}NO_4$: C, 69.28; H, 7.04; N, 4.25; found: C, 69.22; H, 7.06; 4.25; **Minor isomer 34i (syn) *CH*(OMe) signal:** 200 MHz ^1H NMR; δ 4.03 (d, J ≤ 2.0 Hz).

Methyl 3-(2-methoxyphenyl)amino-2-methoxy-3-naphthylpropanoate (33j).

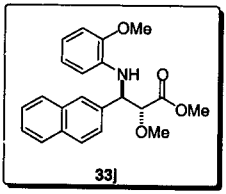

33J

The crude product is a yellow oil which slowly crystallizes and isolated as pale yellow oil which slowly crystallizes as fine yellow needles. Isolated yield: 87%; mp = 103-105 °C; Rf = 0.17 (SiO_2, 25 % hexane/CH_2Cl_2); IR (Thin Film); 3414, 3052, 2998, 2924, 2849, 1744, 1601, 1511, 1457, 1431, 1345, 1272, 1245, 1223, 1132, 1027, 739 cm^{-1}; 200 MHz ^1H

NMR; δ 7.80-7.75 (m, 4H), 7.49-7.40 (m, 3H), 6.78-6.57 (m, 3H), 6.47 (dd, 1H, J = 7.0 Hz, J = 2.0 Hz), 5.47 (bs, 1H), 4.98 (d, 1H, J = 5.0 Hz), 4.28 (d, 1H, J = 5.0 Hz), 3.91 (s, 3H), 3.63 (s, 3H), 3.45 (s, 3H); 50 MHz ^{13}C NMR; δ 170.9, 147.2, 136.3, 136.2, 133.3, 133.2, 128.2, 128.1, 127.7, 126.7, 126.0, 125.9, 125.3, 121.1, 117.3, 111.5, 109.6, 83.9, 59.3, 59.2, 55.6, 52.0. HPLC (gradient # 2): t_R = 13.3 (major diastereomer), t_R = 14.3 (minor diastereomer). An analytical sample was recrystallized from 95% ethanol as fine white needles, analysis calcd for $C_{22}H_{23}NO_4$: C, 72.31; H, 6.34; N, 3.71; found: C, 72.34; H, 6.29; 3.71; **Minor isomer 34j (syn) C*H*(OMe) signal:** 200 MHz ^{1}H NMR; δ 4.15 (d, J = 4.0 Hz).

Methyl 3-(2-methoxyphenyl)amino-2-methoxy-3-(2-furanyl)propanoate (33k).

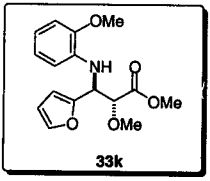

33k

Crude product is dark red oil and is isolated as a red oil, isolated yield: 95%: Rf = 0.11 (SiO_2, 100% CH_2Cl_2); IR (Thin Film); 3402, 2999, 2952, 2835, 1754, 1602, 1511, 1457, 1346, 1272, 1247, 1223, 1179, 1132, 1028, 1011, 740 cm^{-1}; 200 MHz ^{1}H NMR; δ 7.33 (m, 1H), 6.87-6.62 (m, 5H), 6.28-6.24 (m, 1H), 5.03 (d, 1H, J = 4.0 Hz), 4.21 (d, 1H, J = 4.0 Hz), 3.86 (s, 3H), 3.75 (s, 3H), 3.46 (s, 3H); 50 MHz ^{13}C NMR; δ 170.7, 151.8, 147.4, 142.1, 135.9, 121.1, 117.9, 111.6, 110.3, 110.0, 108.0, 81.6, 56.6, 55.5, 53.6, 52.0. HRMS, calcd for $C_{16}H_{19}NO_5$ 305.1263, found 305.1257; HPLC (gradient # 3): t_R = 7.8 (major diastereomer), t_R = 8.4 (minor diastereomer); **Minor isomer 34k (syn) C*H*(OMe) signal:** 200 MHz ^{1}H NMR; δ 4.30 (d, J ≤ 1.0 Hz).

Crystal Structure Data for Esters 33g and 34f.

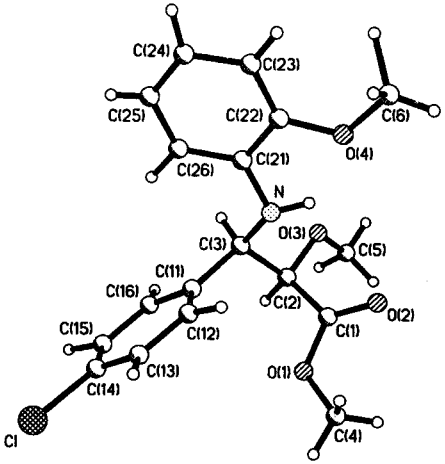

Figure 6. Crystal structure of ester **33g**.

Table 4. Crystal data and structure refinement for ester **33g**.

Identification code	**33g**
Empirical formula	$C_{18}H_{20}ClNO_4$
Formula weight	349.80
Temperature	293(2) K
Wavelength	1.54178 Å
Crystal system, space group	Orthorhombic, Pna2(1)
Unit cell dimensions	a = 11.6442(11) Å alpha = 90 deg.
	b = 19.598(2) Å beta = 90 deg.
	c = 7.9461(6) Å gamma = 90 deg.
Volume	1813.3(3) $Å^{-3}$
Z, Calculated density	4, 1.281 Mg/m^{-3}
Absorption coefficient	2.043 mm^{-1}
F(000)	736
Crystal size	0.48 x 0.18 x 0.10 mm
Theta range for data collection	4.42 to 56.71 deg.
Limiting indices	-12<=h<=12, -21<=k<=21, -8<=l<=8
Reflections collected / unique	2456 / 2249 [R(int) = 0.0267]
Completeness to theta = 56.71	97.0%
Absorption correction	Empirical
Max. and min. transmission	0.3127 and 0.2464
Refinement method	Full-matrix least-squares on F^2

Data / restraints / parameters	2249 / 1 / 270
Goodness-of-fit on F^2	1.003
Final R indices [I>2sigma(I)]	R1 = 0.0473, wR2 = 0.1097
R indices (all data)	R1 = 0.0850, wR2 = 0.1433
Absolute structure parameter	-0.02(4)
Extinction coefficient	0.0021(4)
Largest diff. peak and hole	0.228 and -0.166 eÅ^{-3}

Table 5. Atomic coordinates (x 10^4) and equivalent isotropic displacement parameters (A^2 x 10^3) for **33g**. U(eq) is defined as one third of the trace of the orthogonalized Uij tensor.

	x	y	z	U(eq)
Cl	-1792(2)	-5705(1)	-3504(3)	136(1)
N	-1848(4)	-8604(3)	-8051(6)	64(1)
O(1)	-3549(3)	-8605(2)	-4138(5)	74(1)
C(1)	-3456(5)	-8983(3)	-5530(9)	62(1)
C(2)	-3832(5)	-8587(3)	-7074(7)	58(2)
O(2)	-3086(4)	-9555(2)	-5522(6)	84(1)
O(3)	-4160(3)	-9030(2)	-8379(5)	75(1)
C(3)	-2820(4)	-8164(3)	-7771(8)	59(2)
O(4)	-369(4)	-9541(2)	-8992(6)	88(1)
C(4)	-3094(6)	-8888(4)	-2584(9)	97(2)
C(5)	-5281(5)	-9300(4)	-8154(10)	100(2)
C(6)	442(9)	-10067(6)	-9335(15)	111(3)
C(11)	-2539(4)	-7562(3)	-6647(7)	54(1)
C(12)	-1621(5)	-7554(3)	-5564(8)	64(2)
C(13)	-1407(6)	-6980(4)	-4598(9)	80(2)
C(14)	-2090(7)	-6422(4)	-4720(9)	81(2)
C(15)	-3019(6)	-6418(4)	-5760(10)	83(2)
C(16)	-3226(6)	-6990(3)	-6736(9)	70(2)
C(21)	-977(4)	-8426(3)	-9187(7)	62(2)
C(22)	-183(5)	-8913(4)	-9661(8)	73(2)
C(23)	710(6)	-8750(5)	-10715(11)	97(2)
C(24)	819(9)	-8090(6)	-11282(10)	105(3)
C(25)	62(8)	-7609(7)	-10833(10)	94(3)
C(26)	-865(6)	-7764(4)	-9800(8)	73(2)

Table 6. Bond lengths [Å] and angles [deg] for ester **33g**.

Cl-C(14)	1.740(6)	C(6)-H(6B)	0.97(6)
N-C(21)	1.403(7)	C(6)-H(6A)	1.35(11)
N-C(3)	1.440(7)	C(11)-C(12)	1.372(7)
N-H(1N)	0.85(5)	C(11)-C(16)	1.379(8)
O(1)-C(1)	1.334(7)	C(12)-C(13)	1.384(9)
O(1)-C(4)	1.453(8)	C(12)-H(12)	1.02(5)
C(1)-O(2)	1.201(6)	C(13)-C(14)	1.356(9)
C(1)-C(2)	1.516(8)	C(13)-H(13)	1.02(7)
C(2)-O(3)	1.405(6)	C(14)-C(15)	1.362(10)
C(2)-C(3)	1.543(7)	C(15)-C(16)	1.384(9)
C(2)-H(2)	1.01(5)	C(15)-H(15)	1.27(9)
O(3)-C(5)	1.420(7)	C(16)-H(16)	1.00(6)
C(3)-C(11)	1.515(8)	C(21)-C(22)	1.381(8)
C(3)-H(3)	1.00(5)	C(21)-C(26)	1.392(8)
O(4)-C(22)	1.358(7)	C(22)-C(23)	1.373(9)
O(4)-C(6)	1.424(8)	C(23)-C(24)	1.376(12)
C(4)-H(4A)	0.9600	C(23)-H(23A)	0.9300
C(4)-H(4B)	0.9600	C(24)-C(25)	1.338(12)
C(4)-H(4C)	0.9600	C(24)-H(24)	0.98(8)
C(5)-H(5A)	0.9600	C(25)-C(26)	1.390(10)
C(5)-H(5B)	0.9600	C(25)-H(25)	0.85(6)
C(5)-H(5C)	0.9600	C(26)-H(26)	1.04(4)
C(6)-H(6C)	0.94(6)		

C(21)-N-C(3)	121.2(5)	H(5A)-C(5)-H(5B)	109.5
C(21)-N-H(1N)	106(4)	O(3)-C(5)-H(5C)	109.5
C(3)-N-H(1N)	120(3)	H(5A)-C(5)-H(5C)	109.5
C(1)-O(1)-C(4)	117.6(5)	H(5B)-C(5)-H(5C)	109.5
O(2)-C(1)-O(1)	122.9(6)	O(4)-C(6)-H(6C)	108(4)
O(2)-C(1)-C(2)	125.8(6)	O(4)-C(6)-H(6B)	108(4)
O(1)-C(1)-C(2)	111.3(5)	H(6C)-C(6)-H(6B)	117(6)
O(3)-C(2)-C(1)	111.1(5)	O(4)-C(6)-H(6A)	101(4)
O(3)-C(2)-C(3)	105.9(4)	H(6C)-C(6)-H(6A)	105(6)
C(1)-C(2)-C(3)	110.2(5)	H(6B)-C(6)-H(6A)	116(6)
O(3)-C(2)-H(2)	111(3)	C(12)-C(11)-C(16)	118.3(6)
C(1)-C(2)-H(2)	110(3)	C(12)-C(11)-C(3)	123.2(5)
C(3)-C(2)-H(2)	108(2)	C(16)-C(11)-C(3)	118.5(5)
C(2)-O(3)-C(5)	112.8(5)	C(11)-C(12)-C(13)	119.8(6)
N-C(3)-C(11)	112.8(5)	C(11)-C(12)-H(12)	126(3)
N-C(3)-C(2)	109.5(5)	C(13)-C(12)-H(12)	114(3)
C(11)-C(3)-C(2)	111.8(5)	C(14)-C(13)-C(12)	120.7(6)
N-C(3)-H(3)	111(3)	C(14)-C(13)-H(13)	120(3)
C(11)-C(3)-H(3)	108(3)	C(12)-C(13)-H(13)	119(3)
C(2)-C(3)-H(3)	103(3)	C(15)-C(14)-C(13)	120.9(6)
C(22)-O(4)-C(6)	118.3(7)	C(15)-C(14)-Cl	119.4(7)
O(1)-C(4)-H(4A)	109.5	C(13)-C(14)-Cl	119.7(6)
O(1)-C(4)-H(4B)	109.5	C(14)-C(15)-C(16)	118.3(7)
H(4A)-C(4)-H(4B)	109.5	C(14)-C(15)-H(15)	129(4)
O(1)-C(4)-H(4C)	109.5	C(16)-C(15)-H(15)	113(4)
H(4A)-C(4)-H(4C)	109.5	C(15)-C(16)-C(11)	121.9(7)
H(4B)-C(4)-H(4C)	109.5	C(15)-C(16)-H(16)	121(3)
O(3)-C(5)-H(5A)	109.5	C(11)-C(16)-H(16)	117(3)
O(3)-C(5)-H(5B)	109.5	C(22)-C(21)-C(26)	119.1(6)

C(22)-C(21)-N	119.2(6)	C(24)-C(25)-C(26)	121.0(10)
C(26)-C(21)-N	121.7(6)	C(24)-C(25)-H(25)	130(5)
O(4)-C(22)-C(23)	124.8(7)	C(26)-C(25)-H(25)	109(5)
O(4)-C(22)-C(21)	114.4(5)	C(25)-C(26)-C(21)	118.8(8)
C(23)-C(22)-C(21)	120.8(7)	C(25)-C(26)-H(26)	119(2)
C(24)-C(23)-C(22)	119.2(8)	C(21)-C(26)-H(26)	122(2)
C(24)-C(23)-H(23A)	120.4		
C(22)-C(23)-H(23A)	120.4		
C(25)-C(24)-C(23)	120.9(9)		
C(25)-C(24)-H(24)	132(5)		
C(23)-C(24)-H(24)	107(5)		

Table 7. Anisotropic displacement parameters ($Å^2 \times 10^3$) for ester **33g**. The anisotropic displacement factor exponent takes the form: $-2\pi^2 [(ha^*)^2 U_{11} + ... + 2h\,ka^*b^*U_{12}]$

	U11	U22	U33	U23	U13	U12
Cl	143(2)	137(2)	127(2)	-63(2)	39(2)	-66(1)
N	51(3)	67(3)	72(4)	2(3)	9(3)	9(3)
O(1)	75(3)	84(3)	61(3)	-16(2)	4(2)	10(2)
C(1)	51(3)	69(4)	65(4)	-4(4)	9(3)	-2(3)
C(2)	49(3)	64(4)	62(4)	-18(3)	-4(3)	-3(3)
O(2)	102(3)	69(3)	81(3)	3(3)	12(3)	17(2)
O(3)	59(2)	85(3)	79(3)	-20(3)	-3(2)	-11(2)
C(3)	46(3)	69(4)	62(4)	0(3)	0(3)	3(3)
O(4)	72(3)	87(3)	105(4)	-16(3)	20(3)	19(2)
C(4)	112(6)	114(6)	64(4)	-8(4)	-8(4)	24(5)
C(5)	65(4)	112(5)	123(7)	-30(5)	-4(5)	-23(4)
C(6)	92(6)	116(7)	124(8)	-11(7)	11(6)	28(6)
C(11)	45(3)	59(3)	59(3)	4(3)	-3(3)	-4(3)
C(12)	56(3)	76(4)	59(3)	6(4)	-5(4)	-7(3)
C(13)	67(4)	111(6)	61(4)	-8(4)	-5(4)	-32(4)
C(14)	96(5)	75(5)	72(5)	-24(4)	26(4)	-35(4)
C(15)	85(5)	76(4)	88(5)	-5(4)	13(5)	-7(4)
C(16)	67(4)	71(4)	72(4)	-12(4)	-9(4)	-3(4)
C(21)	50(3)	89(4)	49(3)	-4(3)	2(3)	-6(3)

C(22)	49(3)	100(5)	69(4)	-21(4)	9(3)	-7(4)
C(23)	79(5)	122(7)	90(5)	-33(6)	24(4)	-10(4)
C(24)	87(6)	164(10)	63(5)	-17(6)	17(4)	-27(7)
C(25)	91(6)	127(9)	64(5)	10(6)	-7(5)	-30(6)
C(26)	58(4)	97(5)	62(4)	5(4)	-2(3)	-3(4)

Table 8. Hydrogen coordinates (x 10^4) and isotropic displacement parameters ($Å^2$ x 10^3) for ester **33g**.

	x	y	z	U(eq)
H(1N)	-1950(40)	-9030(20)	-8170(70)	59(18)
H(2)	-4470(40)	-8260(20)	-6770(60)	46(14)
H(3)	-3120(40)	-7980(20)	-88 ^(70'	58(15)
H(4A)	-3214	-8569	-1683	145
H(4B)	-2287	-8972	-2712	145
H(4C)	-3481	-9308	-2331	145
H(5A)	-5464	-9596	-9077	150
H(5B)	-5826	-8933	-8112	150
H(5C)	-5310	-9553	-7120	150
H(6C)	1170(60)	-9910(30)	-8980(90)	90(20)
H(6B)	160(50)	-10490(30)	-8840(90)	90(20)
H(6A)	480(70)	-10050(40)	-11040(140)	160(30)
H(12)	-1080(40)	-7950(20)	-5330(60)	50(14)
H(13)	-700(50)	-6970(30)	-3840(80)	100(20)
H(15)	-3710(70)	-5930(40)	-6070(110)	160(30)
H(16)	-3920(50)	-7010(30)	-7480(80)	74(18)
H(23A)	1236	-9082	-11041	116
H(24)	1480(60)	-8080(40)	-12050(110)	110(30)
H(25)	10(50)	-7200(30)	-11140(90)	90(30)
H(26)	-1450(40)	-7380(20)	-9500(50)	33(11)

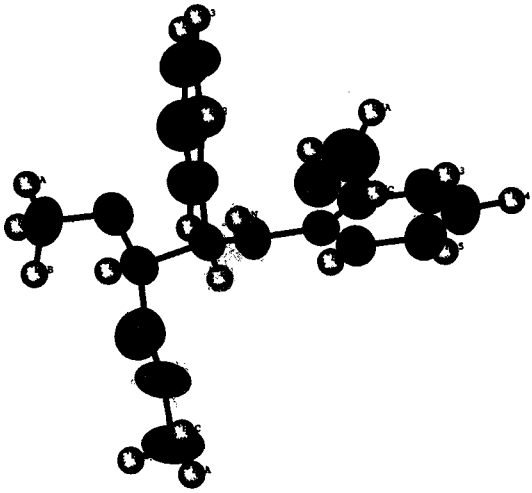

Figure 7. Crystal structure of ester **34f**.

Table 9. Crystal data and structure refinement for ester **34f**.

Identification code	**34f**
Empirical formula	C18 H21 N O4
Formula weight	315.36
Temperature	566(2) K
Wavelength	1.54178 Å
Crystal system, space group	Monoclinic, P2(1)/c
Unit cell dimensions	a = 11.9067(10) Å alpha = 90 deg.
	b = 16.6101(12) Å beta = 104.162(9)deg.
	c = 8.9888(8) Å gamma = 90 deg.
Volume	1723.7(2) $Å^{-3}$
Z, Calculated density	4, 1.215 Mg/m^{-3}
Absorption coefficient	0.701 mm^{-1}
F(000)	672
Crystal size	0.20 x 0.45 x 0.35 mm
Theta range for data collection	3.83 to 54.96 deg.
Limiting indices	-12<=h<=12, -17<=k<=17, -9<=1<=9
Reflections collected / unique	7895 / 2147 [R(int) = 0.1087]
Completeness to theta = 54.96	99.2 %
Absorption correction	Empirical

Max. and min. transmission	0.6621 and 0.5146
Refinement method	Full-matrix least-squares on F^2
Data / restraints / parameters	2147 / 0 / 293
Goodness-of-fit on F^2	1.011
Final R indices [I>2sigma(I)]	R1 = 0.0394, wR2 = 0.1174
R indices (all data)	R1 = 0.0424, wR2 = 0.1228
Extinction coefficient	0.0036(5)
Largest diff. peak and hole	0.111 and -0.127 $e.A^{-3}$

Table 10. Atomic coordinates (x 10^4) and equivalent isotropic displacement parameters ($Å^2$ x 10^3) for **34f**. U(eq) is defined as one third of the trace of the orthogonalized Uij tensor.

	x	y	z	U(eq)
N	2560(2)	4301(1)	75(2)	60(1)
O(1)	1583(1)	4942(1)	3121(2)	87(1)
C(1)	2673(2)	4894(1)	3026(2)	65(1)
O(2)	3384(1)	4475(1)	3816(2)	88(1)
C(2)	2873(2)	5440(1)	1765(2)	59(1)
O(3)	4054(1)	5467(1)	1792(1)	75(1)
C(3)	2215(2)	5130(1)	192(2)	54(1)
O(4)	3727(1)	3098(1)	-628(2)	79(1)
C(4)	1272(3)	4433(3)	4278(4)	112(1)
C(5)	4719(3)	5935(2)	3023(3)	97(1)
C(6)	4412(3)	2435(2)	-891(5)	106(1)
C(11)	2387(2)	5683(1)	-1082(2)	57(1)
C(12)	3319(2)	5602(1)	-1727(2)	76(1)
C(13)	3468(2)	6117(2)	-2863(3)	95(1)
C(14)	2690(3)	6715(2)	-3372(3)	101(1)
C(15)	1766(3)	6815(2)	-2747(3)	100(1)
C(16)	1611(2)	6296(1)	-1610(2)	78(1)
C(21)	2000(2)	3810(1)	-1130(2)	55(1)
C(22)	2607(2)	3147(1)	-1496(2)	63(1)
C(23)	2084(3)	2618(1)	-2643(3)	84(1)
C(24)	948(2)	2742(2)	-3437(3)	91(1)
C(25)	347(2)	3383(2)	-3090(2)	82(1)
C(26)	870(2)	3918(1)	-1944(2)	65(1)

Table 11. Bond lengths [Å] and angles [deg] for ester **34f**.

N-C(21)	1.389(2)	C(6)-H(6C)	1.01(3)
N-C(3)	1.448(2)	C(11)-C(12)	1.379(3)
N-H(1N)	0.80(2)	C(11)-C(16)	1.379(3)
O(1)-C(1)	1.323(2)	C(12)-C(13)	1.378(3)
O(1)-C(4)	1.457(3)	C(12)-H(12)	0.94(2)
C(1)-O(2)	1.188(2)	C(13)-C(14)	1.359(4)
C(1)-C(2)	1.516(3)	C(13)-H(13)	1.01(3)
C(2)-O(3)	1.401(2)	C(14)-C(15)	1.362(4)
C(2)-C(3)	1.528(2)	C(14)-H(14)	0.86(3)
C(2)-H(2)	1.023(16)	C(15)-C(16)	1.383(3)
O(3)-C(5)	1.424(3)	C(15)-H(15)	0.95(3)
C(3)-C(11)	1.519(2)	C(16)-H(16)	0.95(2)
C(3)-H(3)	1.005(17)	C(21)-C(26)	1.377(3)
O(4)-C(22)	1.372(2)	C(21)-C(22)	1.400(2)
O(4)-C(6)	1.424(3)	C(22)-C(23)	1.382(3)
C(4)-H(4A)	0.96(3)	C(23)-C(24)	1.381(3)
C(4)-H(4C)	0.96(5)	C(23)-H(23)	0.90(2)
C(4)-H(4B)	0.95(3)	C(24)-C(25)	1.362(4)
C(5)-H(5C)	1.05(4)	C(24)-H(24)	1.00(3)
C(5)-H(5B)	0.98(3)	C(25)-C(26)	1.387(3)
C(5)-H(5A)	0.95(3)	C(25)-H(25)	0.96(2)
C(6)-H(6B)	0.96(3)	C(26)-H(26)	0.92(2)
C(6)-H(6A)	0.99(3)		

C(21)-N-C(3)	121.62(15)	H(5C)-C(5)-H(5B)	98(3)
C(21)-N-H(1N)	114.6(14)	O(3)-C(5)-H(5A)	109.1(17)
C(3)-N-H(1N)	114.2(14)	H(5C)-C(5)-H(5A)	117(3)
C(1)-O(1)-C(4)	115.8(2)	H(5B)-C(5)-H(5A)	115(2)
O(2)-C(1)-O(1)	124.34(18)	O(4)-C(6)-H(6B)	101(2)
O(2)-C(1)-C(2)	125.27(19)	O(4)-C(6)-H(6A)	106.0(18)
O(1)-C(1)-C(2)	110.39(16)	H(6B)-C(6)-H(6A)	114(3)
O(3)-C(2)-C(1)	110.31(15)	O(4)-C(6)-H(6C)	104.6(18)
O(3)-C(2)-C(3)	108.17(14)	H(6B)-C(6)-H(6C)	113(3)
C(1)-C(2)-C(3)	110.58(15)	H(6A)-C(6)-H(6C)	117(3)
O(3)-C(2)-H(2)	108.2(8)	C(12)-C(11)-C(16)	117.85(18)
C(1)-C(2)-H(20	110.8(8)	C(12)-C(11)-C(3)	121.89(16)
C(3)-C(2)-H(2)	108.7(8)	C(16)-C(11)-C(3)	120.25(17)
C(2)-O(3)-C(5)	113.33(18)	C(11)-C(12)-C(13)	120.9(2)
N-C(3)-C(11)	115.24(14)	C(11)-C(12)-H(12)	117.4(12)
N-C(3)-C(2)	107.30(14)	C(13)-C(12)-H(12)	121.5(12)
C(11)-C(3)-C(2)	111.16(14)	C(14)-C(13)-C(12)	120.2(3)
N-C(3)-H(3)	108.5(9)	C(14)-C(13)-H(13)	122.5(16)
C(11)-C(3)-H(3)	109.4(9)	C(12)-C(13)-H(13)	117.3(16)
C(2)-C(3)-H(3)	104.6(9)	C(13)-C(14)-C(15)	120.2(2)
C(22)-O(4)-C(6)	117.9(2)	C(13)-C(14)-H(14)	122.0(17)
O(1)-C(4)-H(4A)	104.9(19)	C(15)-C(14)-H(14)	117.6(17)
O(1)-C(4)-H(4C)	106(3)	C(14)-C(15)-C(16)	119.7(3)
H(4A)-C(4)-H(4C)	132(4)	C(14)-C(15)-H(15)	122.8(18)
O(1)-C(4)-H(4B)	104.0(18)	C(16)-C(15)-H(15)	117.2(19)
H(4A)-C(4)-H(4B)	120(3)	C(15)-C(16)-C(11)	121.1(2)
H(4C)-C(4)-H(4B)	87(3)	C(15)-C(16)-H(16)	120.6(13)
O(3)-C(5)-H(5C)	105.9(18)	C(11)-C(16)-H(16)	118.2(13)
O(3)-C(5)-H(5B)	111.0(17)	C(26)-C(21)-N	123.97(16)

C(26)-C(21)-C(22)	118.07(16)
N-C(21)-C(22)	117.91(16)
O(4)-C(22)-C(23)	125.76(18)
O(4)-C(22)-C(21)	113.50(15)
C(23)-C(22)-C(21)	120.7(2)
C(24)-C(23)-C(22)	119.8(2)
C(24)-C(23)-H(23)	122.0(15)
C(22)-C(23)-H(23)	118.2(15)
C(25)-C(24)-C(23)	120.1(2)
C(25)-C(24)-H(24)	121.7(15)
C(23)-C(24)-H(24)	118.3(14)
C(24)-C(25)-C(26)	120.3(2)
C(24)-C(25)-H(25)	122.6(14)
C(26)-C(25)-H(25)	116.9(14)
C(21)-C(26)-C(25)	121.0(2)
C(21)-C(26)-H(26)	116.8(12)
C(25)-C(26)-H(26)	122.2(13)

Table 12. Anisotropic displacement parameters ($Å^2 \times 10^3$) for ester **34f**. The anisotropic displacement factor exponent takes the form: $-2\pi^2 [(ha^*)^2 U_{11} + ... + 2h\, ka^* b^* U_{12}]$

	U11	U22	U33	U23	U13	U12
N	62(1)	57(1)	55(1)	-4(1)	7(1)	6(1)
O(1)	86(1)	111(1)	73(1)	24(1)	35(1)	18(1)
C(1)	75(1)	64(1)	52(1)	-4(1)	9(1)	5(1)
O(2)	89(1)	84(1)	82(1)	22(1)	2(1)	6(1)
C(2)	71(1)	57(1)	51(1)	-3(1)	17(1)	5(1)
O(3)	71(1)	93(1)	60(1)	-13(1)	11(1)	-7(1)
C(3)	58(1)	55(1)	50(1)	-2(1)	13(1)	6(1)
O(4)	82(1)	65(1)	92(1)	-1(1)	22(1)	17(1)
C(4)	108(2)	158(3)	80(2)	30(2)	41(2)	-6(2)
C(5)	98(2)	114(2)	70(2)	-17(1)	6(1)	-36(2)
C(6)	122(2)	74(2)	127(3)	12(2)	40(2)	36(2)
C(11)	64(1)	58(1)	46(1)	-4(1)	9(1)	1(1)
C(12)	84(1)	78(2)	71(1)	9(1)	28(1)	7(1)
C(13)	104(2)	107(2)	83(2)	10(1)	40(1)	-14(2)
C(14)	128(2)	100(2)	72(2)	28(2)	19(2)	-19(2)
C(15)	115(2)	90(2)	89(2)	31(1)	11(2)	13(2)
C(16)	83(1)	82(2)	68(1)	14(1)	15(1)	14(1)
C(21)	69(1)	53(1)	44(1)	4(1)	17(1)	-5(1)
C(22)	80(1)	53(1)	59(1)	3(1)	23(1)	-3(1)
C(23)	121(2)	59(1)	78(2)	-8(1)	38(2)	-4(1)
C(24)	115(2)	79(2)	74(1)	-11(1)	14(1)	-26(2)
C(25)	84(2)	90(2)	66(1)	1(1)	6(1)	-19(1)
C(26)	70(1)	70(1)	55(1)	0(1)	13(1)	-5(1)

Table 13. Hydrogen coordinates (x 10^4) and isotropic displacement parameters ($Å^2$ x 10^3) for ester **34f**.

	x	y	z	U(eq)
H(2)	2602(12)	6014(10)	1903(17)	46(4)
H(3)	1378(15)	5139(9)	228(18)	55(4)
H(4A)	440(30)	4484(18)	4100(30)	139(11)
H(4C)	1760(40)	3970(30)	4370(50)	210(20)
H(4B)	1760(30)	4618(17)	5220(40)	119(10)
H(5C)	4250(30)	6470(20)	3040(40)	158(13)
H(5B)	4660(30)	5717(18)	4020(40)	140(11)
H(5A)	5480(30)	5983(17)	2910(30)	125(10)
H(6B)	5140(30)	2560(20)	-190(40)	141(13)
H(6A)	4430(20)	2467(19)	-1980(40)	133(11)
H(6C)	4020(30)	1950(20)	-570(40)	140(11)
H(12)	3806(17)	5158(13)	-1420(20)	74(6)
H(13)	4150(20)	6021(16)	-3300(30)	124(9)
H(14)	2780(20)	7058(16)	-4050(30)	103(8)
H(15)	1170(30)	7197(18)	-3120(30)	129(10)
H(16)	950(19)	6339(13)	-1210(20)	86(6)
H(23)	2503(19)	2201(14)	-2850(30)	92(7)
H(24)	590(20)	2352(17)	-4260(30)	118(8)
H(25)	-430(20)	3507(13)	-3650(20)	89(7)
H(26)	488(17)	4358(13)	-1690(20)	74(6)
H(1N)	3239(18)	4225(12)	360(20)	66(6)

References

1. For biological applications of ß-amino acids see Griffith, O. W. in *Ann. Rev. Biochem.* **1986**, 55, 855.

2. Borman, S., *Chem. Eng. News.* **1991,** 69(35), 11. Miller, R. W. *J. Nat. Prod.* **1980**, 43, 425.

3. Tanner, D., Somfai, P. *Tetrahedron* **1988**, 44, 613 and 619.

4. Ojima, I., Inaba, S., Yoshida, K. *Tetrahedron Letters.* **1977**, 41, 3643-3646.

5. Ishitani, H., Ueno, M., Kobayashi, S. *J. Am. Chem. Soc.* **1997**, 119, 7153-7154.

6. Annunziata, R., Cinquini, M., Cozzi, F., Cozzi, P. G., *J. Org. Chem.* **1992**, 57, 4155-4162.

7. Abrahams, I., Motevalli, M., Robinson, A. J. Wyatt, P. B. *Tetrahedron.* **1994**, 50, 12755-12772.

8. Adrian, J. C., Jr., Chick, J. Unpublished Results

9. Annunziata, R., Cinquini, M., Cozzi, R., Borgia, A. L.,*J. Org. Chem.* **1992**, 57, 6339-6342.

10. Fujisawa, T., Shimizu, M. *Tetrahedron Letters.* **1993**, 34, 1307-1310.

11. Adrian, J. C., Jr., Barkin, J. L., Hassib, L. *Tetrahedron Letters.* **1999**, 40, 2457-2460.

12. Evans, D. A., Urpi, F., Somers, T. C., Clark, J. S., Bilodeau, M. T. *J. Am. Chem. Soc.***1990**, 112, 8215-8216.

13. Zimmerman, H. E., Traxler, M. D. *J. Am. Chem. Soc.* **1957**, 79, 1920.

14. Still, W. C., Khan, M., Mitra, A. *J. Org. Chem.* **1978**, 43, 2923-2925.

Figure 9a. ^{1}H NMR

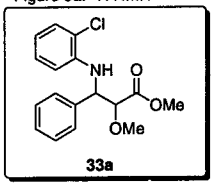

33a

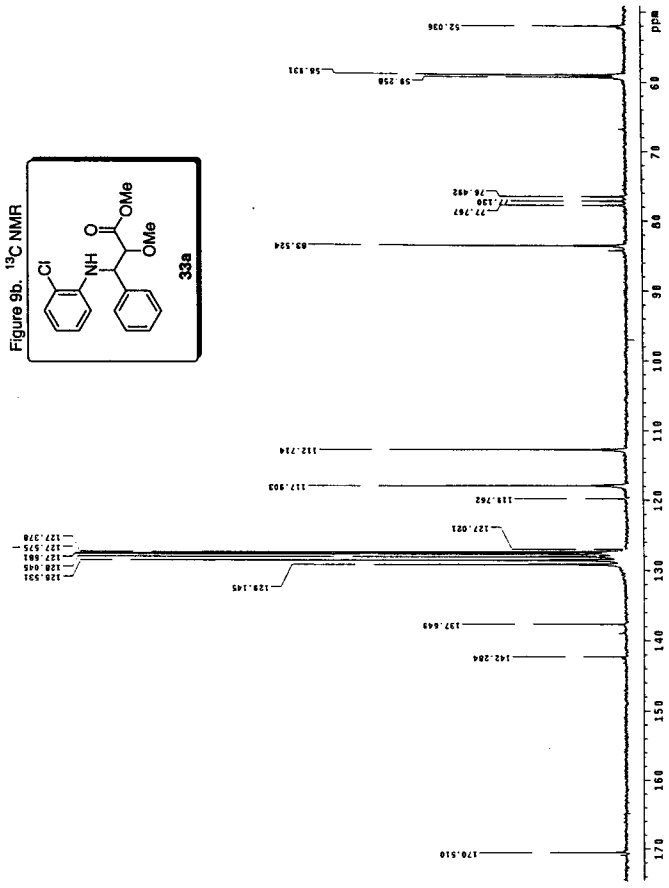

Figure 9b. ^{13}C NMR

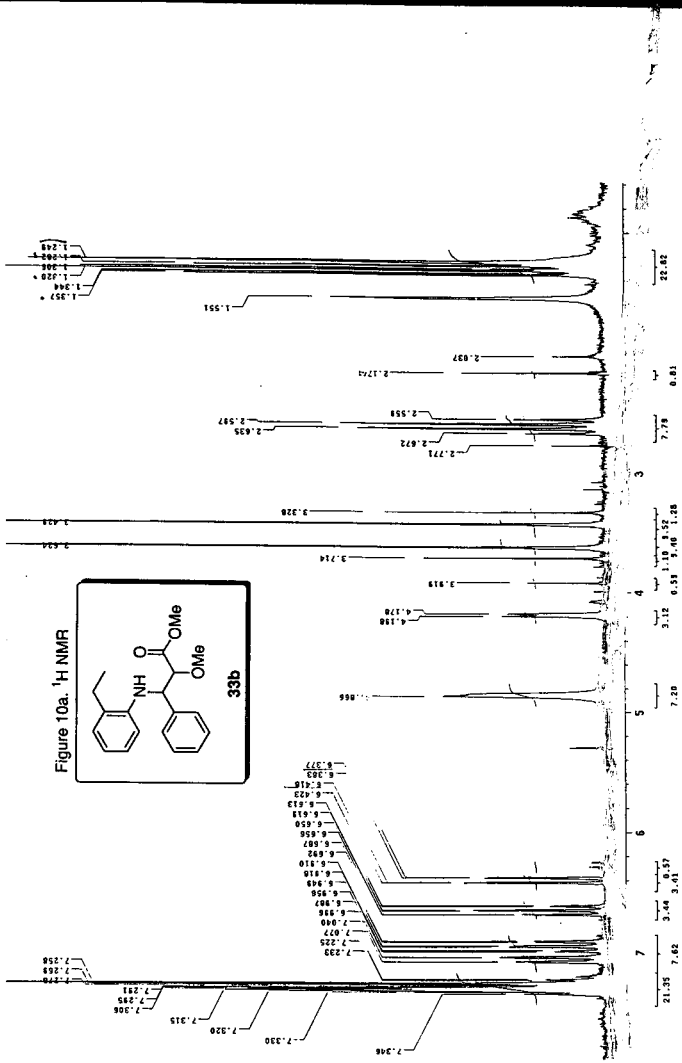

Figure 10a. ^{1}H NMR

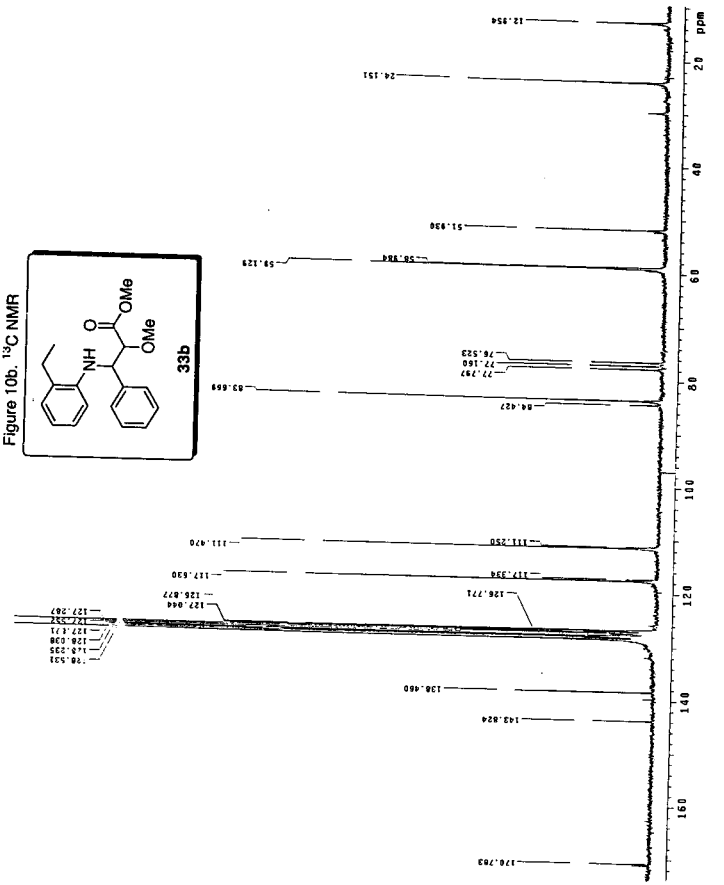
Figure 10b. ^{13}C NMR
33b
OMe
OMe
NH
O
ppm
20
40
60
80
100
120
140
160
12.954
24.151
51.930
56.586
59.129
76.529
77.160
77.797
83.669
86.627
111.250
111.470
117.334
117.630
126.772
126.827
127.064
127.267
127.532
127.671
128.038
128.235
128.531
136.460
143.824
170.763

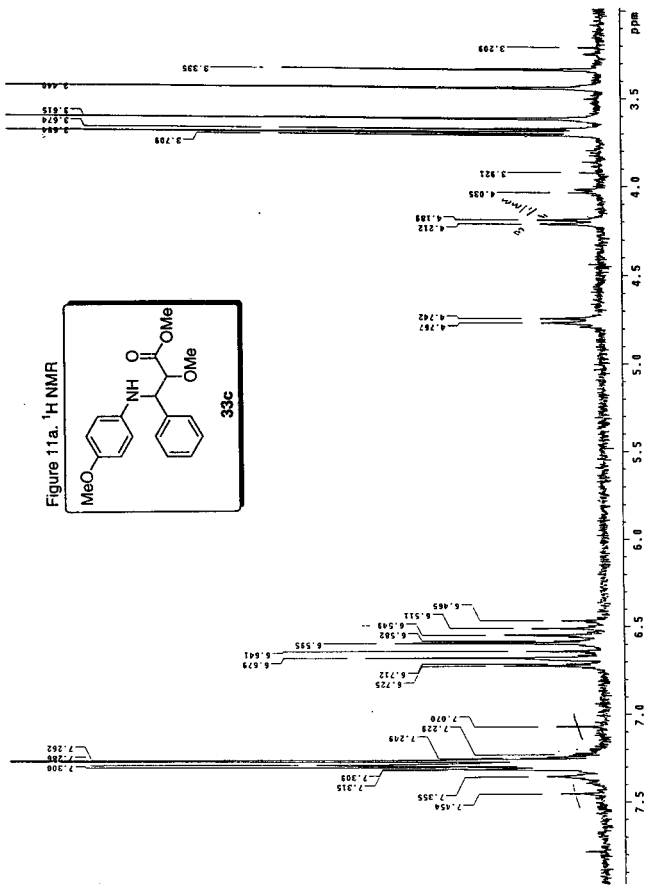

Figure 11a. ^{1}H NMR

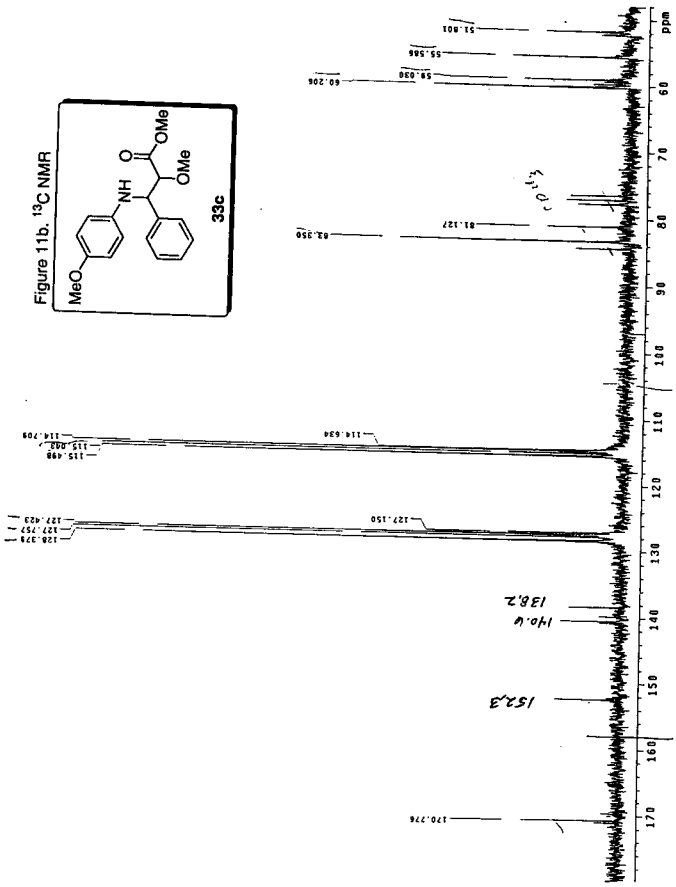
Figure 11b. ^{13}C NMR
MeO
NH
OMe
OMe
33c
170.776
152.3
140.4
138.2
127.150
126.379
127.757
127.023
116.636
115.498
115.002
114.709
83.350
81.127
60.206
59.038
55.566
51.801
ppm

Figure 12a. ^{1}H NMR

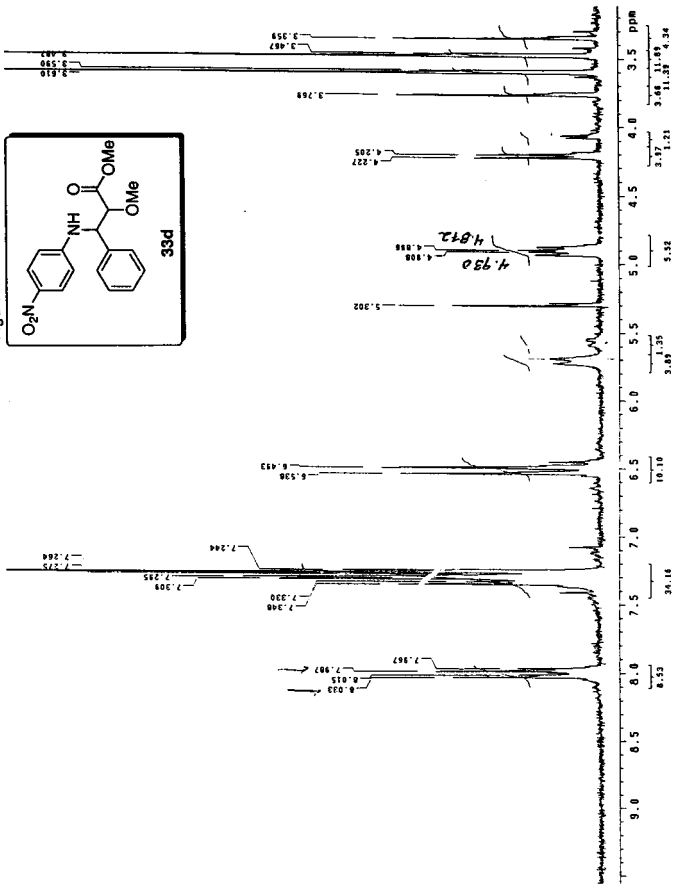

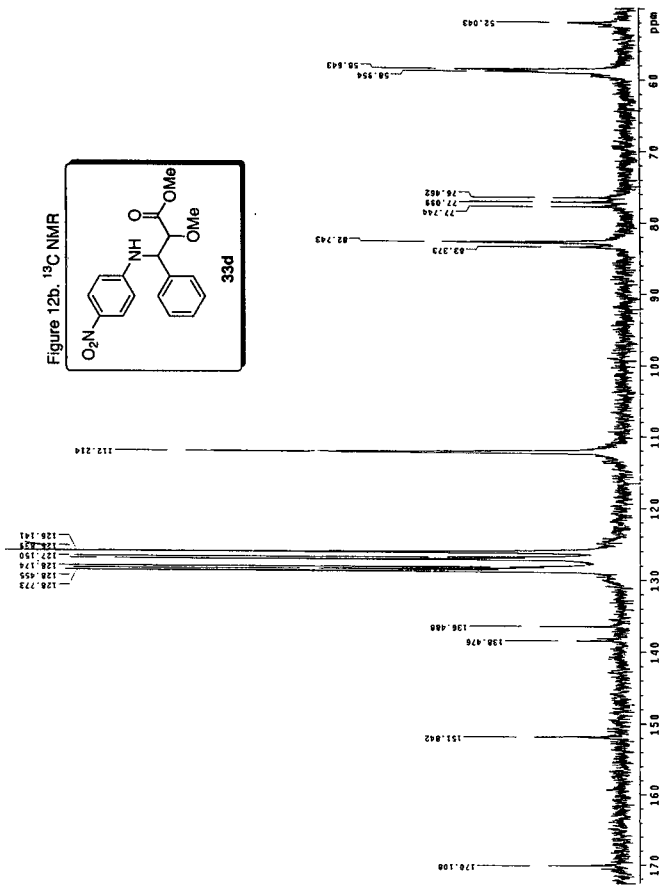
Figure 12b. ^{13}C NMR
33d
OMe
OMe
NH
O_2N
170.108
151.842
136.476
136.466
129.773
128.655
128.174
127.150
126.829
126.141
112.214
82.743
77.744
77.099
76.462
63.373
58.643
58.554
52.043
ppm

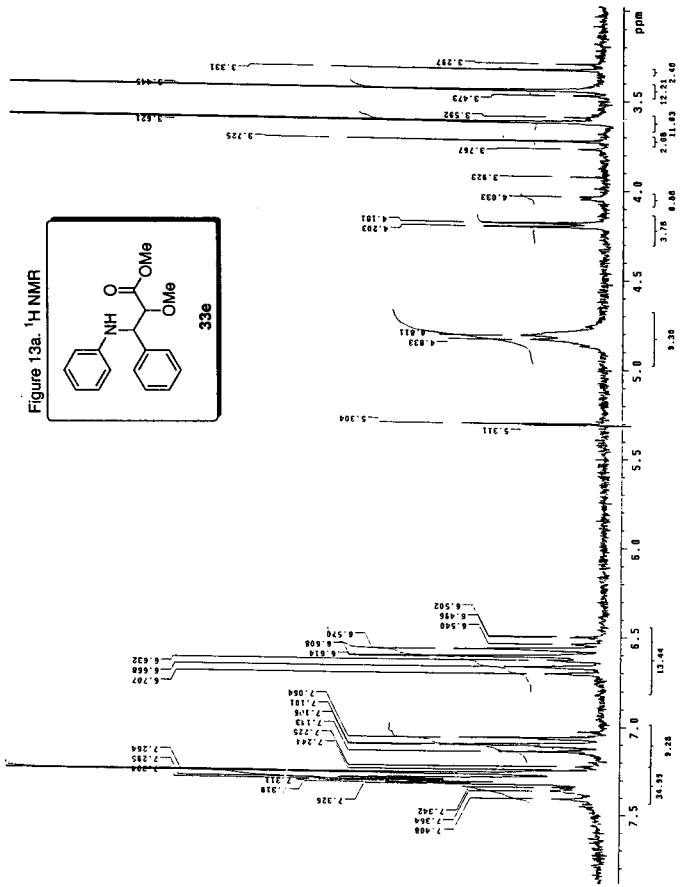

Figure 13a. ^{1}H NMR

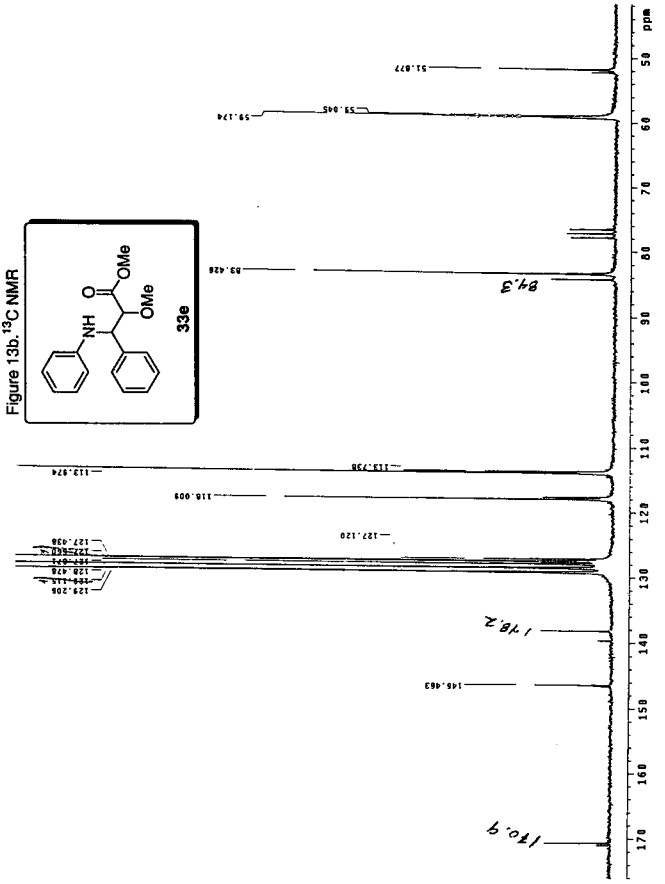

Figure 13b. ^{13}C NMR

Figure 14a. ^{1}H NMR

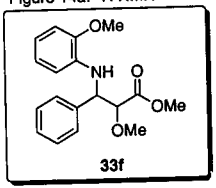

33f

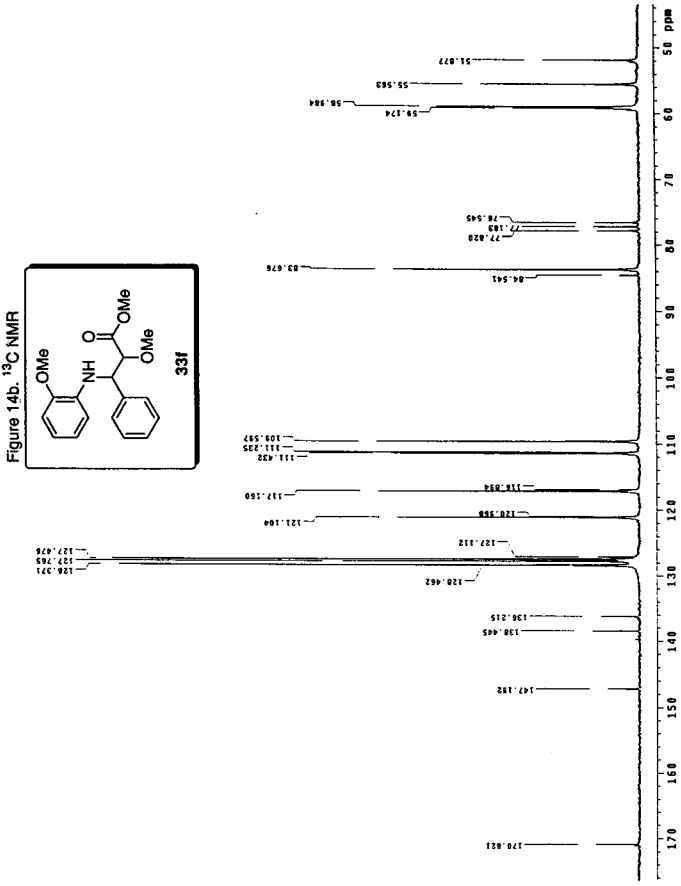
Figure 14b. ^{13}C NMR
OMe
NH
O
OMe
OMe
33f
51.827
55.563
58.984
59.124
77.020
77.183
78.545
83.676
84.541
105.537
111.235
111.432
117.150
118.094
120.558
121.104
127.112
127.478
127.765
128.021
128.462
136.215
138.445
147.192
170.821
50
60
70
80
90
100
110
120
130
140
150
160
170
ppm

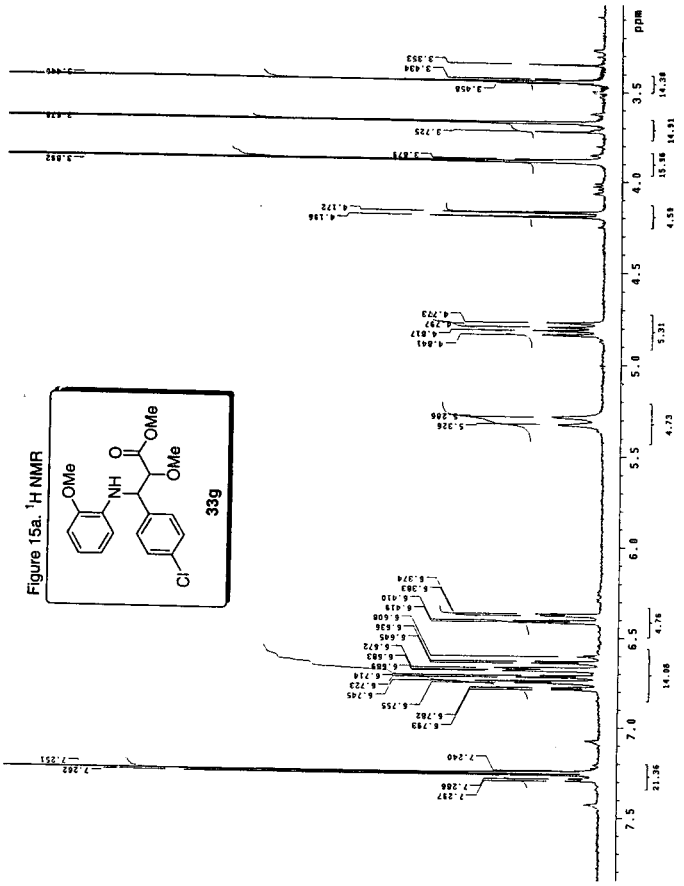
Figure 15a. ^{1}H NMR
OMe
NH
O
OMe
OMe
Cl
33g
ppm

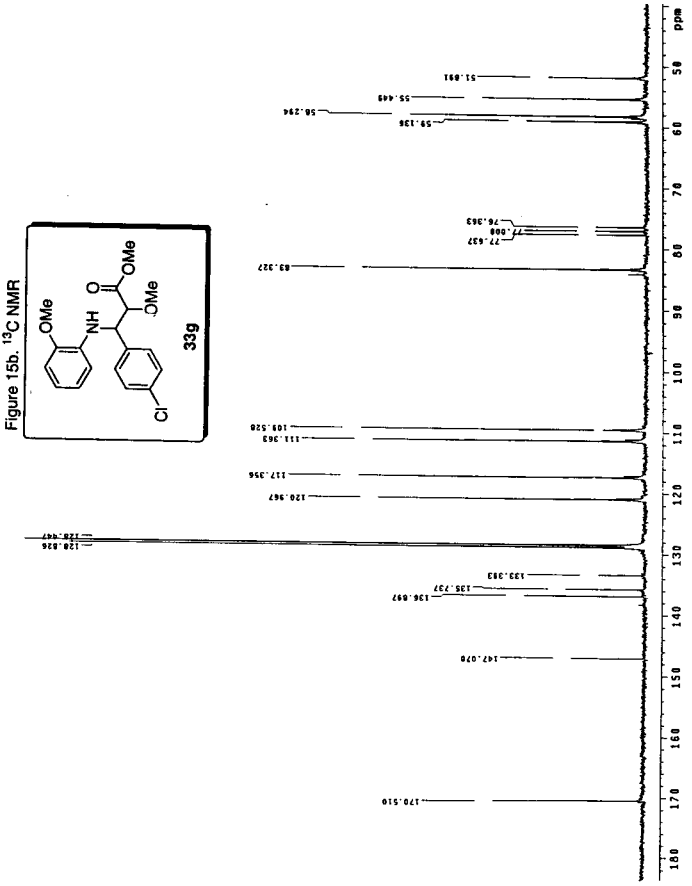

Figure 15b. ^{13}C NMR

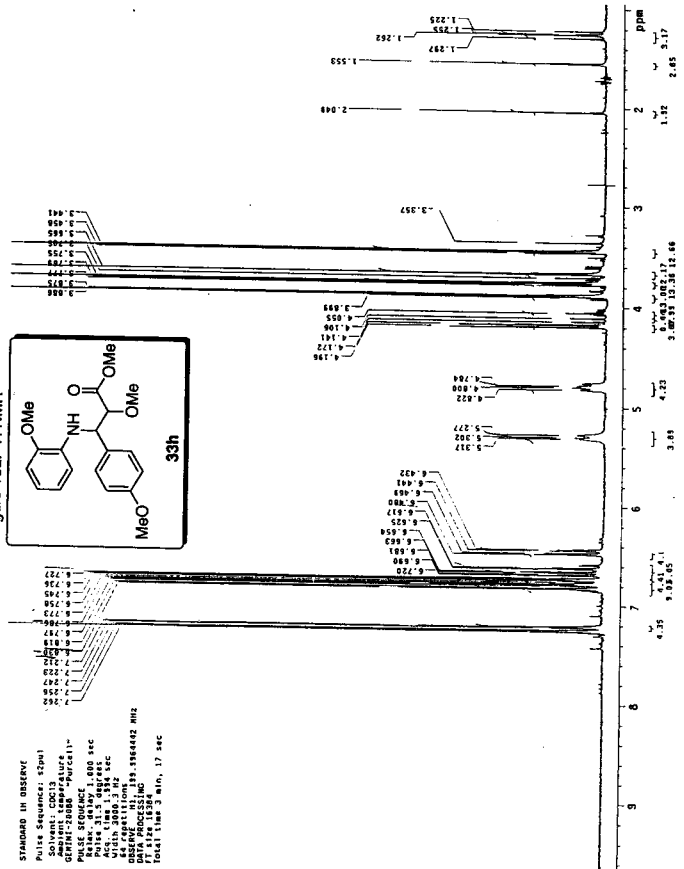

Figure 16a. ^{1}H NMR

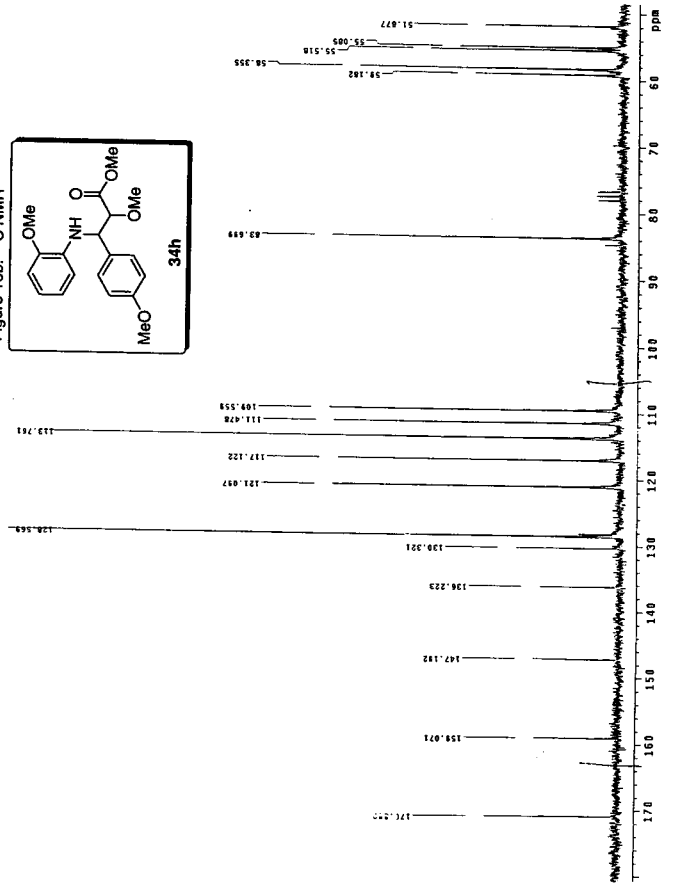

Figure 16b. ^{13}C NMR

Figure 17a. ^{1}H NMR

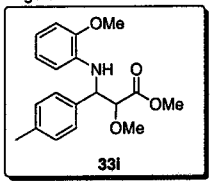

33i

Figure 17b. ^{13}C NMR

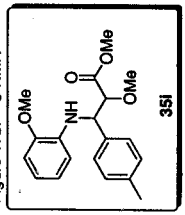

Figure 18a. ^{1}H NMR

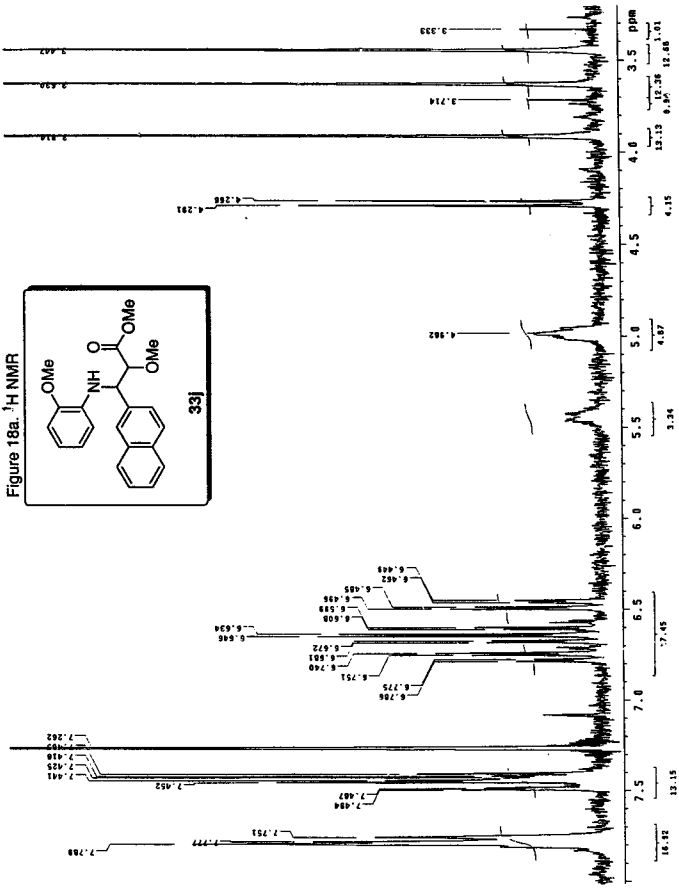

Figure 18b. ^{13}C NMR

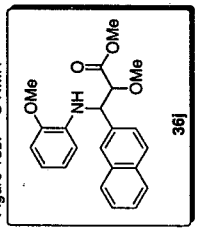

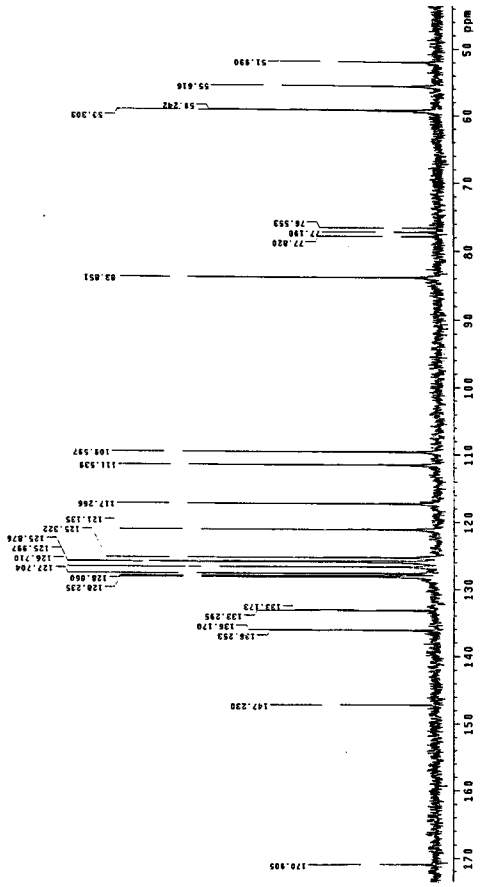

Figure 19a. ^{1}H NMR

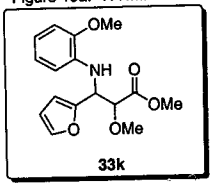

33k

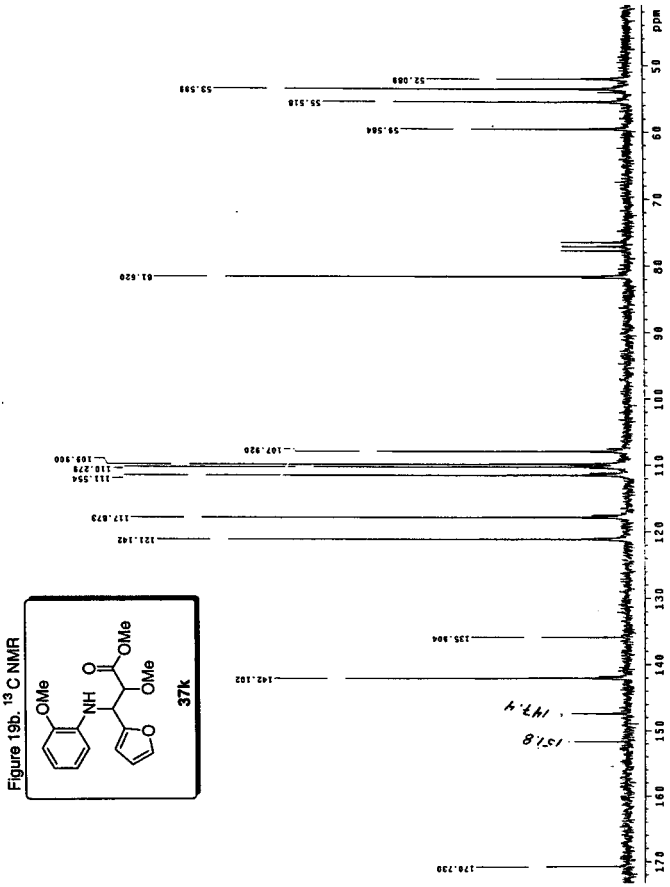

Figure 19b. ^{13}C NMR

Figure 20. ^{1}H NMR